1995-06

Implementation of a fiber-optic code-division multiple access data link

McKown, Kenneth J.

Monterey, California. Naval Postgraduate School

NAVAL POSTGRADUATE SCHOOL
Monterey, California

THESIS

IMPLEMENTATION OF A FIBER-OPTIC CODE-DIVISION MULTIPLE ACCESS DATA LINK

by

Kenneth J. McKown

June 1995

Thesis Advisor: John P. Powers

Approved for public release; distribution is unlimited.

REPORT DOCUMENTATION PAGE

Form Approved OMB No. 0704

1. AGENCY USE ONLY *(Leave blank)*	2. REPORT DATE June 1995	3. REPORT TYPE AND DATES COVERED Master's Thesis

4. TITLE AND SUBTITLE
IMPLEMENTATION OF A FBER-OPTIC CODE-DIVISION MULTIPLE ACCESS DATA LINK

5. FUNDING NUMBERS

6. AUTHOR(S) MCKOWN, Kenneth J.

7. PERFORMING ORGANIZATION NAME(S) AND ADDRESS(ES)
Naval Postgraduate School
Monterey CA 93943-5000

8. PERFORMING ORGANIZATION REPORT NUMBER

9. SPONSORING/MONITORING AGENCY NAME(S) AND ADDRESS(ES)

10. SPONSORING/MONITORING AGENCY REPORT NUMBER

11. SUPPLEMENTARY NOTES
The views expressed in this thesis are those of the author and do not reflect the official policy or position of the Department of Defense or the U.S. Government.

12a. DISTRIBUTION/AVAILABILITY STATEMENT
Approved for public release; distribution is unlimited

12b. DISTRIBUTION CODE

13. ABSTRACT *(maximum 200 words)*

This thesis was a continuance study on the feasibility of implementing a code division multiple access scheme which utilizes optical fiber delay lines. This report explores pseudo-orthogonal address codes with aperiodic correlation properties for on-off signaling. The optical functions such as code sequence generation and correlation are performed by parallel optic delay lines acting as encoders and decoders. This experiment shows the desired auto-correlation and cross-correlation properties of these codes and their use in FO-CDMA. The results were recorded and analyzed. This scheme allows for a large population of simultaneously communicating users on a single network unit and allows enhanced flexibility in the scope of services that a local area server can provide.

14. SUBJECT TERMS
Fiber Optics, CDMA , Multiple Access, Spread Spectrum, Delay Lines

15. NUMBER OF PAGES
80

16. PRICE CODE

17. SECURITY CLASSIFICATION OF REPORT	18. SECURITY CLASSIFICATION OF THIS PAGE	19. SECURITY CLASSIFICATION OF ABSTRACT	20. LIMITATION OF ABSTRACT
Unclassified	Unclassified	Unclassified	UL

NSN 7540-01-280-5500

Standard Form 298 (Rev. 2-89)
Prescribed by ANSI Std. 239-18

Approved for public release; distribution is unlimited.

IMPLEMENTATION OF A FIBER-OPTIC CODE-DIVISION MULTIPLE ACCESS DATA LINK

Kenneth J. McKown
Lieutenant, United States Navy
B.A. Chemistry/Mathematics, California State University Fresno, 1986

Submitted in partial fulfillment
of the requirements for the degree of

MASTER OF SCIENCE IN ELECTRICAL ENGINEERING

from the

NAVAL POSTGRADUATE SCHOOL
June 1995

Author: [redacted]
Kenneth J. McKown

Approved by: [redacted]
John P. Powers, Thesis Advisor

[redacted]
Ron J. Pieper, Second Reader

[redacted]
Michael A. Morgan, Chairman
Department of Electrical and Computer Engineering

ABSTRACT

This thesis was a continuance study on the feasibility of implementing a code division multiple access scheme which utilizes optical fiber delay lines. This report explores pseudo-orthogonal address codes with aperiodic correlation properties for on-off signaling. The optical functions such as code sequence generation and correlation are performed by parallel optic delay lines acting as encoders and decoders. This experiment shows the desired auto-correlation and cross-correlation properties of these codes and their use in FO-CDMA. The results were recorded and analyzed. This scheme allows for a large population of simultaneously communicating users on a single network unit and allows enhanced flexibility in the scope of services that a local area server can provide.

TABLE OF CONTENTS

I. INTRODUCTION 1

A. SPREAD SPECTRUM 1

B. SPREAD SPECTRUM SIGNALS 3

C. DIRECT SEQUENCE 3

D. FREQUENCY HOPPING 5

E. OPTICAL FIBER 6

F. THESIS OBJECTIVES 6

II. CDMA DESIGN 8

A. SYSTEM OVERVIEW 8

B. BASIC CDMA SEQUENCE 9

1. M-Sequences 11

2. Gold Sequences 11

3. Optical Orthogonal Code Sequences 13

C. POWER BUDGET OF PSO CODES. 15

III. SYSTEM OVERVIEW 18

A. DESIGN 18

B. CDMA COMPONENTS 21

1. Bit rate. 21

2. Source 22

3 Detector 22

4. Pattern Generator 23

5. Oscilloscope 24

6. Fiber 25

7. Power Budget 25

IV. ENCODERS 28

A. DESIGN 28

B. CONSTRUCTION 30
C. PERFORMANCE 32
V. DECODERS 36
A. DESIGN 36
B. CONSTRUCTION 38
VI. RESULTS 41
A. AUTO-CORRELATION 41
B. CROSS-CORRELATION 42
C. SIMULTANEOUS OPERATION 48
D. THRESHOLD DETECTOR 52
VII. SUMMARY 58
APPENDIX A. E/O CONVERSION CHART 61
APPENDIX B. MEASURED SPLITTING LOSSES 63
APPENDIX C. MATLAB SOURCE CODE 65
LIST OF REFERENCES 69
INITIAL DISTRIBUTION LIST 71

I. INTRODUCTION

A. SPREAD SPECTRUM

There is a communications revolution in progress today. The tremendous increased demand for communications produces a need for the efficient use of the frequency spectrum. Efficient spectrum use and its diverse applications has stimulated research in spread spectrum.

In spread spectrum the means of transmission for a signal occupies a bandwidth in excess of the minimum required to send information. The band spread is obtained by a code which is independent of the transmitted data. The despread and data recovery is accomplished by a synchronized reception with the code at the receiver.

An important parameter of spread spectrum systems is the number of orthogonal signaling formats that could be used to communicate a data symbol. This number (which is often referred to as the "multiplicity factor" of the communication link) is also known as the "processing gain". Spread spectrum systems typically have multiplicity factors in the thousands. Although standard modulation schemes such as AM, FM and PCM spread the spectrum, the processing gain is near unity and therefore do not qualify as spread spectrum.

Due to the nature of their signal characteristics, there are many advantages for spread spectrum [Ref. 1: p. 882].

1. An antijam capability can be secured with an unpredictable carrier signal. A well-designed spread spectrum system forces a jammer to guess which of the orthogonal signaling formats is being used. Due to the high processing gain this is very difficult, if not impossible.
2. Cryptographic capabilities result from the carrier modulation being effectively random to an unwanted observer.
3. Code division multiple access (CDMA) systems that utilize transmitter-receiver pairs can minimize co-channel interference. This system provides the ability for

two or more users to communicate simultaneously when each user is given a distinct sequence that identifies that user.

4. Low probability of intercept (LPI) can be achieved with high processing gain and unpredictable carrier signals when power is spread thinly and uniformly in the frequency domain. This makes detection against noise by a receiver difficult.

From the listed advantages it is easy to see that applications for the spread spectrum continue to be a primary concern for the military. However, with the increasing demands for mobile radio networks, timing and positioning systems, and specialized satellite applications, the private sector has taken a very strong interest in using spread spectrum techniques.

There are many types of spread spectrum systems (SS). To be considered an SS system, a system must satisfy two criteria [Ref. 2: p. 449].

1. The bandwidth of the transmitted signal, *s(t)*, needs to be much greater than that of the message, *m(t)*.
2. The relatively wide bandwidth of *s(t)* must be caused by an independent modulating waveform, *c(t)*, (called the *spreading signal*), and this signal must be known by the receiver in order for the message signal, *m(t)*, to be detected.

The complex envelope of the spread spectrum signal is a function of both *m(t)* and *c(t)*. In most cases a product function is used so that:

$$g(t) = g_m(t)g_c(t). \tag{1}$$

Here $g_m(t)$ and $g_c(t)$ are the usual types of modulation functions that generate FM, PM, AM, etc. [Ref. 2: p. 449].

B. SPREAD SPECTRUM SIGNALS

Spread spectrum systems are classified by the techniques which they employ to achieve the wideband carrier signal. Some examples of common spread spectrum techniques are [Ref. 1, p. 824]:

1. Direct sequence (DS) systems that employ pseudo-random sequences, phase-shift keyed (PSK) onto the carrier for spreading.
2. Frequency hopping (FH) systems that drive a frequency synthesizer with a pseudo-random sequence of numbers, thereby producing carrier spreading .

Due to the simplicity, efficiency and excellent resolution, direct sequence was considered to be the optimal choice for this thesis.

C. DIRECT SEQUENCE

The direct sequence technique spreads the spectrum by modulating the original signal with a very wideband signal (relative to the data bandwidth). Thus, the spread spectrum signal is dominated by the spreading signal which is nearly independent of the data signal [Ref. 3, p. 69]. The wideband signal has two possible amplitudes (± 1) which are switched in a pseudo-random manner.

The complex envelope for a spread spectrum signal in the case of BPSK modulation is given by [Ref. 2: p. 450]:

$$g(t) = A_c m(t) c(t) \tag{2}$$

where $m(t)$ is the message signal and $g(t)$ is a polar spreading signal. When a pseudo-noise code generator is used, the values of $c(t)$ are ± 1. The output signal $s(t) = Re\{g(t)e^{j\omega_c t}\}$ is the binary-phase-shift-keyed data, direct sequence spreading, spread spectrum signal (BPSK-DS-SS) [Ref. 2: p. 450].

Figure 1 is a block diagram of the BPSK-DS-SS transmitter. The signal is first modulated and then the spectrum is spread. If a digital signal rate is 2.5 Kb/s, for example,

the resulting BPSK-modulated signal bandwidth is 5.0 KHz. The bandwidth may then spread to 15 MHz (for example). The ratio between the two frequencies is the processing gain and, in this case, it is equal to 3,000 [Ref. 3: p. 70].

Figure 2 is the block diagram of the BPSK-DS-SS receiver. The spread signal is remodulated with the same spreading code generator which has the effect of despreading. The resulting signal is demodulated in the normal way. The message signal is obtained from the filtered demodulated signal. This process produces excellent resolution and is efficient in power amplification which makes it very attractive for communications.

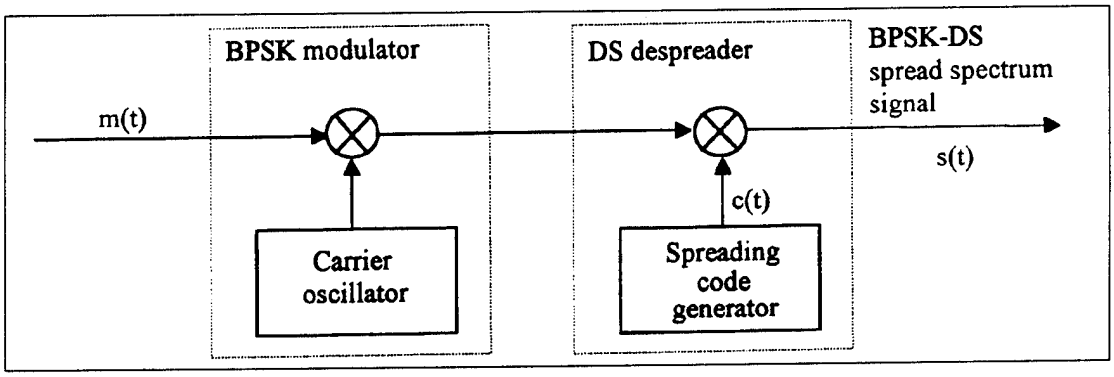

Figure 1. BPSK-DS-SS Transmitter. [After Ref. 2: p. 451]

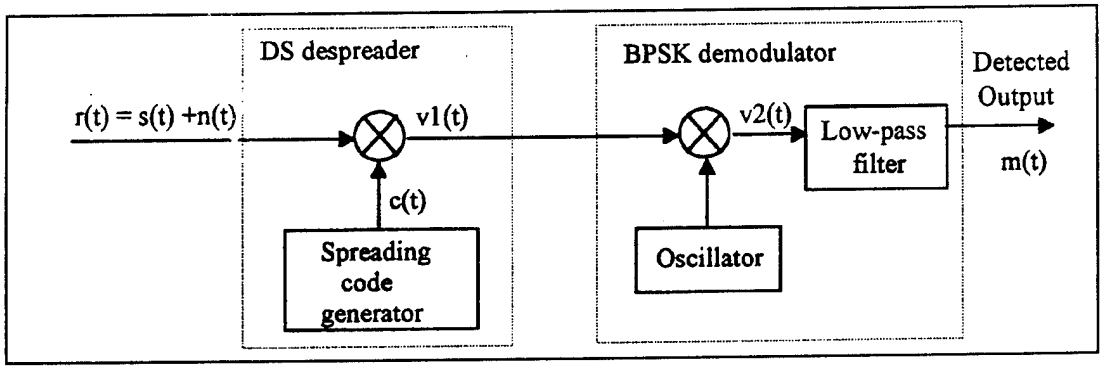

Figure 2. BPSK-DS-SS Receiver. [After Ref. 2: p. 451]

D. FREQUENCY HOPPING

Frequency hopping (FH) systems produces a carrier spreading by driving a frequency synthesizer with a pseudo-random sequence of numbers spanning the range of the synthesizer [Ref. 1: p. 824].

Figure 3 shows the frequency-hopped spread spectrum (FH-SS) system. There are $M = 2^k$ hop frequencies where k chip words are taken to determine each hop frequency. The frequency hopping is accomplished by a mixer. The serial-to-parallel converter reads k chip parallel words.

Figure 4 is the block diagram of the FH-SS receiver. The receiver must have the same spreading code *c(t)* so the receiver can be synchronized with the transmitter. The data is recovered from the dehopped signal by FSK or BSK demodulator.

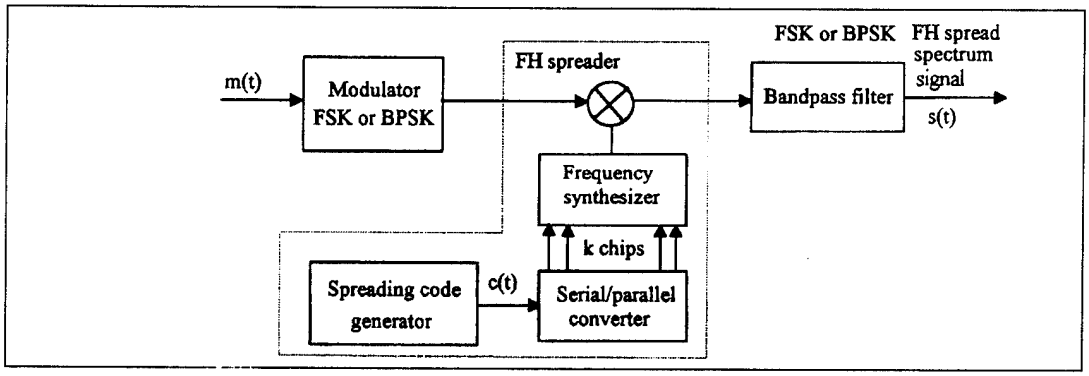

Figure 3. FH-SS Transmitter. [After Ref. 2: p. 457]

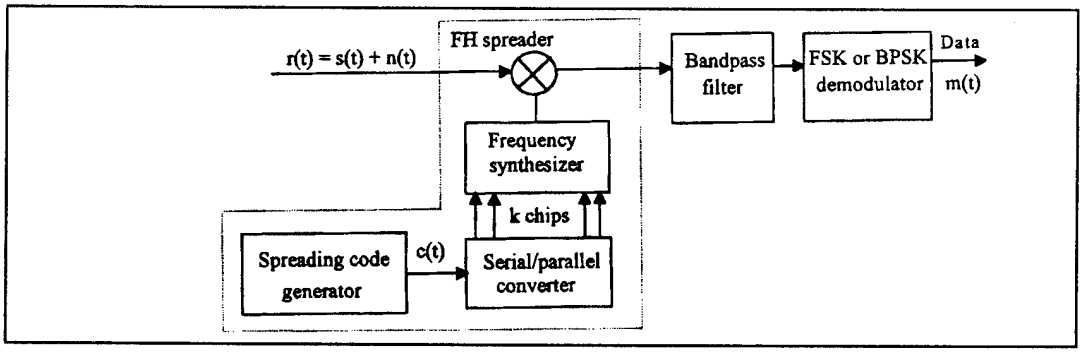

Figure 4. FH-SS Receiver. [After Ref. 2: p. 457]

The processing gain is the product of the hop time and the frequency range. For this reason this spread spectrum system produces the highest multiplicity factor and therefore is optimum for antijamming applications.

E. OPTICAL FIBER

Because of the ability to handle large amounts of information, optical fibers are rapidly becoming the primary choice for communication networks. As incredible as these advancements have been, only a small fraction of the available bandwidth is utilized. This is no surprise because the usable bandwidth is as much as 50 THz or 50,000 GHz [Ref. 4: p. 370]. In the fastest presently operating terrestrial system, the rate is 1.7 Gb/s, while in TAT-8, each fiber carries just a few hundred Mb/s [Ref. 5: p. 29]. The bottleneck is then the required electronic signal conversion. Furthermore, the use of multiple channels is generally considered too cumbersome and costly with conventional systems. Clearly, the solution is to exploit the spread spectrum bandwidth by utilizing an all-optical approach.

The performance attributes of spread spectrum systems include low probability of intercept, antijam and multiple user random access communications with selective addressing (CDMA) and accurate universal timing. The means by which these applications are achieved is through optical fibers.

F. THESIS OBJECTIVES

The objective of this thesis was a continuance study on the feasibility of implementing a code division multiple access scheme which utilizes optical fiber delay lines. The preliminary groundwork on this subject was done by Andre [Ref. 6]. The optical functions, such as coded sequence generation and correlation, were performed by parallel optic delay lines acting as encoders and decoders. Figure 5 depicts the schematic of the system that was implemented. The performance of this communication scheme was to be analyzed in terms of the system's parameters such as number of users, weight, length of

the address codes, laser power and fiber length. The intent was to redesign Andre's code division multiple access system by decreasing the optical pulsewidth by a factor of one-tenth of that used in the preliminary experiments and also to implement a threshold detector. Thus, at the receiver end the original data was regenerated.

An important note to make is the format of this thesis is similar to Reference [6]. This was done for easy comparison of results. The ultimate goal is to show that a successful CDMA system can be implemented using a pulsewidth of 5 ns.

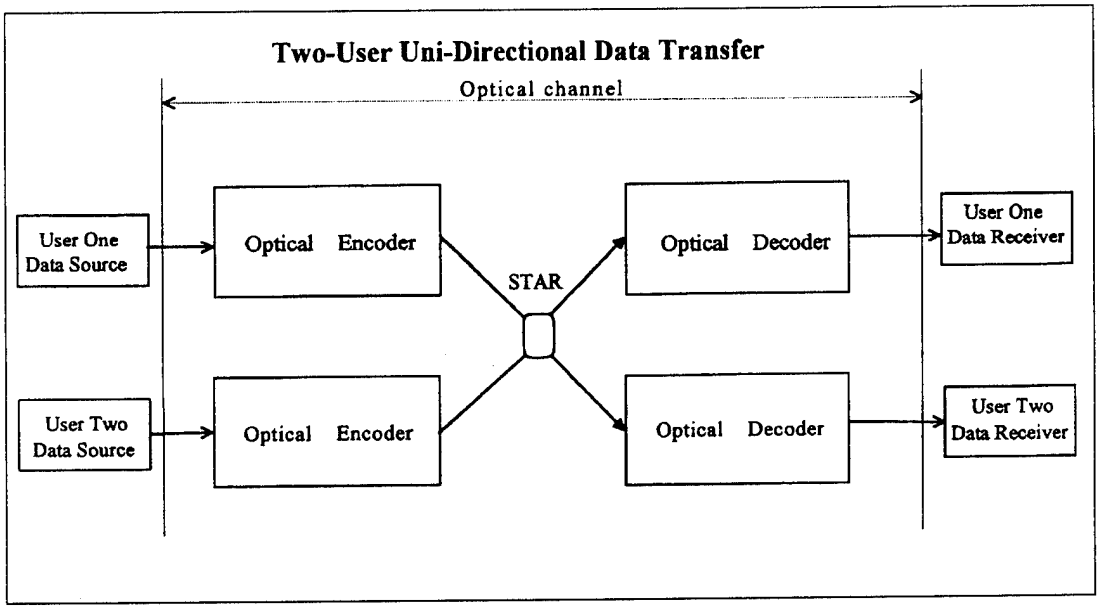

Figure 5. CDMA Schematic with Optical Encoding and Decoding. [After Ref. 1: p. 824]

II. CDMA DESIGN

A. SYSTEM OVERVIEW

There are many advantages to using fiber optics for communications. The most important advantage is the high data rates which can be achieved. Fiber optic code division multiple access takes advantage of this excess bandwidth by mapping a low information rate of electrical or optical signals into a high rate of optical pulse sequences to provide communication access to many users.

In communication systems employed today, a system of optical pulses in optical fibers are converted to electrical signal for the desired signal-processing. The pulses are then converted back to optical signals and transferred to the next destination. This system is therefore limited to electronic rates and not optical. In order to achieve higher speed of optical signal processing, the electronic data rate conversion needs to be limited. The optimal system would be a pure optical scheme that exploits the extremely large bandwidth of the optical fiber. This system would fully integrate optical components and have the ability to perform signal processing functions optically. Ultimately this scheme offers higher speed and is more efficient then conventional systems.

The goal is to provide asynchronous access to each user, thus making efficient use of the channel and permitting users to have simultaneous access with no waiting time. To make this system feasible, the address of each user must be assigned orthogonal codes. This maximizes the auto-correlation function and minimizes the cross-correlation function.

The selection of sets of pulse sequence is a main concern in code design. The set of optimal sequences that possess both minimal levels of pairwise cross-correlation and minimal levels of off-peak auto-correlation are designated as pseudo-orthogonal (PSO) codes. Pulse position modulation is chosen due to its ability to reduce channel cross-talk.

To generate the desired pulse sequences, a pulse is sent through a parallel set of fiber optic delay lines. These delay lines are selected to provide the proper spacing

between pulses in the sequence. The resultant light pulse sequence is then transmitted over the fiber lines to the final destination.

The receiver is another set of delay lines that are inversely matched to the encoder delay lines. The received signals pass through the decoder which acts a correlator. The output sequence reaches the highest peak level when the sequence exactly fills the correlator and is aligned perfectly. Thus, the original signal is recovered at the desired station.

The proposed system takes advantage of the extremely large bandwidth of optical fibers by the construction of pure optical components. These optical components perform the correlation functions that are routinely done by electronic means. The signal conversion from the optical to electrical domain is done sparingly and, therefore, the speed of the system is vastly increased.

B. BASIC CDMA SEQUENCE

Each bit in a CDMA system is encoded into a waveform $s(t)$ that corresponds to a code sequence of k chips. Each receiver correlates its own code address $f(t)$ with the received signal $s(t)$. The receiver output $r(t)$ can be written as [Ref. 7 : p. 547]

$$r(t) = \int_{-\infty}^{+\infty} s(t) f(z - t)\, dz. \tag{3}$$

If the signal has arrived at the correct destination, then $s(t)$ is equal to $f(t)$ and Eq. 3 is the auto-correlation function. However, if $s(t)$ is not equal $f(t)$ (meaning that the signal has arrived at the unintended destination), then Eq. 3 represents the cross-correlation of the functions. By selecting the proper set of coded sequences, the cross-correlation function is minimized while the auto-correlation function is maximized. The discrimination between signal and interference at each receiver is therefore maximized.

In CDMA, many asynchronous users can occupy the same channel simultaneously. Each user's receiver must extract its own information in the presence of others. This information is referred to as a signature sequence on which information data bits of different users are mapped. Each set of signature sequences that are distinguishable from time shifted versions of themselves. Consider the following two periodic signals [Ref. 1: p. 825]

$$x(t) = \frac{1}{T_c} \sum_{n=-\infty}^{\infty} x_n P_{T_c}(t - nT_c) \tag{4}$$

and

$$y(t) = \frac{1}{T_c} \sum_{n=-\infty}^{\infty} y_n P_{T_c}(t - nT_c). \tag{5}$$

Here P_{Tc} is a unit rectangular pulse of duration T_c. The periodic sequences x_n and y_n have a period of $F = T/T_c$. The primary concern in design is constructing sequences that satisfy the following two conditions [Ref. 1: p. 825].

1. For any sequence $x = (x_n)$ the auto-correlation is given by:

$$|Z_{x,x}(l)| = \left| \sum_{n=0}^{F-1} x_n x_{n+l} \right| = \begin{cases} K \text{ for } l = 0 \\ \leq \lambda_a \text{ for } 1 \leq l \leq F-1 \end{cases} \tag{6}$$

2. For each pair of sequences $x = (x_n)$ and $y = (y_n)$, the cross-correlation is given by:

$$|Z_{x,y}(l)| = \left| \sum_{n=0}^{F-1} x_n y_{n+l} \right| = \lambda_c \text{ for } 0 \leq l \leq F. \tag{7}$$

The values of K, λ_c and λ_a are all constants. If $\lambda_c = \lambda_a = 0$, then the sequences are strictly orthogonal. However, in reality, λ_c and λ_a will have some nonzero value. The purpose in using orthogonal codes is to minimize λ_c and λ_a. The auto-correlation is maximum at $l = 0$ and at any other value it is a minimum.

In general the designed sequences that satisfy Eq. 6 and 7 are optical orthogonal codes of length F, weight K with auto-correlation and cross-correlation constraints, λ_c and λ_a.

1. M-Sequences

M-sequences (or minimal length) sequences are shift register sequence of length (or period) $N = 2^n - 1$ (which is the longest sequence length an n-stage binary linear feedback shift register can generate). A characteristic of the m-sequence code is its two-valued discrete auto-correlation function which is given by [Ref. 7: p. 548]:

$$r(t) = \begin{cases} N \text{ for } t = 0 \\ -1 \text{ for } t = i\frac{T}{N},\ i = \pm 1; \pm 2, \cdots \end{cases} \tag{8}$$

where T is the data bit width. Although the maximal length sequence is easy to distinguish from the time shifted version of itself, the peak of the cross correlation is not less than $-1 + 2^n$. This causes certain maximal length sequences to interfere very strongly with each other. This strong interference and the fact that maximal length sequence sets are few in number makes m-sequences impractical for CDMA.

1. Gold Sequences

The cross-talk (interference) component in the code multiplex transmission system cannot be made less than $-1 + 2^{(n+1)}$ [Ref. 8: p.21]. The size of the maximal set of m-sequence which has this bound (i.e., the size of the set where every two elements are a

preferred pair) is not very large. In Reference [8], a detailed proof shows that in reality there cannot be more than six addresses if only *m*-sequences are used.

Gold sequences are generated by combining a pair of preferred maximal length sequences using modulo-2 addition [Ref. 7: p. 548]. The characteristic of the preferred pair are not changed even though their out-of-phase auto-correlation magnitude is larger than that of the *m*-sequence. Suppose a and b is a preferred pair with length N (= 2^n-1; n = odd number). The Gold sequence set is given by [Ref. 7: p. 548]:

$$G(a,b) = \{a, b, a \oplus b, a \oplus Sb, a \oplus S^2b, \cdots, a \oplus S^{N-1}b \qquad (9)$$

where S is a phase shift operator which shifts sequences to the left by one place, a and b are one-period sequences of length N,and $\oplus$ is the shift operation.

Assuming synchronization between transmitter and receiver and considering other user's interference to be the dominant source of noise in the system, the SNR for Gold sequences is [Ref. 7: p. 549]:

$$SNR_{\text{conventional}} = 4\left(\frac{N^3}{(k-1)(N^2+N-1)}\right) \qquad (10)$$

where k is the number of users and N the number of chips. For a given number of chips per bit, the SNR decreases as the number of users increase. In other words, as more and more users access the network at a given time, the system degrades rapidly. To accommodate the increase in number of simultaneous users, the number of chips per bit must be increased. This implies that this processing is ultimately limited by the speed of electronics.

3. Optical Orthogonal Code Sequences

For CDMA to function correctly, a proper set of optimal sequences must be selected. The sequences that posses a minimal level of pairwise correlation and minimal level of off-peak auto-correlation are designated as pseudo-orthogonal (PSO) codes. The level of the transmitted optical code sequence for incoherent optical processing corresponds to light "ON" or light "OFF" [Ref. 7, p. 549]. In the correct code sequence a "0" symbol corresponds to the light "OFF" while a "1" corresponds to the light "ON". The (0,1) sequence is a sequence of ones and zeros of a given finite length. For practicality the length of these sequences must be held to a minimum while maintaining an acceptable correlation behavior. For Gold codes, the number in each coded sequence varies and, therefore, so does the peak of the auto-correlation function. This makes Gold codes less than optimum for incoherent optical processing and thus a poor choice for the orthogonal set [Ref. 1 p.17].

Consider two (0,1) sequences of length L, $\underline{X} = (x_1, x_2,...,x_L)$ and $\underline{Y} = (y_1,y_2,...,y_L)$ where x_i and y_i are either a one or a zero. Assuming both sequences contain n ones (sequence "weight"), with n less than or equal to L, the correlation of $\underline{X}$ and $\underline{Y}$ is [Ref. 9, p. 2]:

$$C_{X,Y}(t) = \sum_{i=1}^{L} x_i y_i + \varepsilon \tag{11}$$

where t takes on integer values and the product is real multiplication. The auto-correlation of $\underline{X}$ is defined when $\underline{X}$ is equal to $\underline{Y}$ and the cross-correlation is defined when $\underline{X}$ is not equal to $\underline{Y}$. Since each product term is either a one or a zero, the peak of the auto-correlation of the (0,1) sequence is the code weight.

A "pseudo-orthogonal (0,1) code set" is one in which all members have auto-correlation and cross-correlations satisfying the following conditions [Ref. 9, p. 3]:

$$C_{X,X}(t) = \begin{cases} n, & t = 0 \\ \leq 1, & t \neq 0 \end{cases} \qquad (12)$$

$$C_{X,Y}(t) = \leq 1 \text{ for all } t.$$

Each sequence has a weight $n > 0$; this implies that there must some t such that $C_{X,Y}(t)$ is at least one. This means that there exists a shift in Y so that its ones are in alignment with X at least once and that there is at least one value of t (t not equal to zero), such that $C_{X,X}(t) > 1$. Thus the pseudo-orthogonal code set never exceeds the longest minimum value for its cross-correlation and off-peak auto-correlation function [Ref. 9: p. 3].

The key, then, is to find a coded sequence such that there exists no repeated spacing among the pulse-pairs. If this is true then the auto-correlation condition in Eq. 11 is guaranteed. Furthermore, the cross-correlation in Eq. 12 is also guaranteed. The relationship between the sequence length L, the sequence weight n and the number of sequences in the code set r is given as [Ref. 9: p. 4]:

$$L \geq \frac{rn(n-1)}{2} + 1. \qquad (13)$$

The minimum length of the largest sequence is found from the above equation, where each sequence contains n ones.

The code set selected for this thesis is an aperiodic pseudo-orthogonal code set. The correlation is based upon a single period of each sequence which is surrounded by all zeros. By convention the minimum value of the separation of pulses in a given sequence is denoted as $g(r,n)$, where r is the number of members and n is the number of pulses. With the aid of a computer the solution for the optimum two user system is given as [Ref. 9: p. 7]:

$$g(r,4) = \begin{cases} 6r, & r = 1,\ 4 \le r \le 15 \\ 6r+1, & r = 2,\ 3 \end{cases} \tag{14}$$

For simplicity, r was chosen as 2 for this thesis, meaning that the minimum sequence length was 14 with a code weight of 4. Table 1 depicts the graphical representation of Eq. 14.

Table 1. Sequence Solution Set. [Ref. 9: p. 20]

Pulse Locations for				
User	*g(2,4)*			
1	1	4	13	14
2	1	6	8	12

This sequence set was the basis for the system design and implementation of a two-user system with sequence codes of length 14. The sequence set represents a set of pulse modulated signals with the pulse in the first slot serving as the reference pulse. The following pulses identify the code word by their spacing from the first.

C. POWER BUDGET OF PSO CODES

The previous sections outlined the theory of pulse coded sequences. The delay lines are used to generate unique code sequence which identifies each source. The data recovered is achieved by optical correlation for sequence recognition.

The basic limitations of CDMA is the inherent power robbing due to the sum of many signals simultaneously modulating over a limited laser dynamic range and the power loss subjected by the parallel fiber optic delay lines encountered.

The laser pulse is split into each of n delay line of the respective encoder and recombined, thus producing a power loss of $1/n^2$ where n is the code weight. The

recombined sequence is sent through the system to each destination. This process is repeated when sent through the decoder. The total propagation loss from the laser output to the photodetector is [Ref. 10: p. 23]:

$$\text{loss} = \left(1/n^4\right)(1/r)\ F_L \tag{15}$$

where the first term is the incoherent encoder-decoder split and combined losses. The coupling loss is $1/r$ and F_L is the fiber transmission loss. If the laser average power is P_a, and the length of the sequence is divided into a number of equal time intervals (pulsewidth of the laser), then the peak pulse power after M number of slots per modulation is [Ref. 10, p. 23]:

$$P_p = LMP_a \tag{16}$$

Here M is the number of designated interval slots for the CDMA sequence and L is the total length of the sequence. In CDMA the desired optical pulse sequence arrives at the receiver and passes through the correlator. The output light intensity traces out the correlation function of the particular sequence and reaches a peak value when the sequence exactly fills the correlator. Defining the photodetector input pulse power as P_r, the correlator then integrates n correct sequence pulses to form a light pulse of power nP_r. An understanding in the system power loss is necessary in selecting the laser. The pulse laser must produce sufficient power to overcome the noise and the CDMA system losses.

The key to a successfully operating CDMA system is the choice of the specific code-words used to generate the spreading signals that provide orthogonal properties between each signal. The set of optimal sequences that possess both minimal levels of pairwise cross-correlation and minimal levels of off-peak auto-correlation are designated as pseudo-orthogonal (PSO) codes. Although there are many different sequences that

satisfy this condition, the (0,1) optical orthogonal code sequence provides the optimal solution and therefore was chosen for this thesis. The proceeding chapters develops a scheme to implement these sequences into a communication system.

III. SYSTEM OVERVIEW

A. DESIGN

The incoherent optic CDMA system implemented in this thesis utilizes (0,1) pulse sequences. The sequence sets corresponds to pulsed waveforms with on-off pulsed signaling application. Figure 6 shows the detailed diagram of this CDMA system design in a star configuration. The set of optical sequences becomes a set of address codes or signature codes for the network. The goal of this scheme is for each user to extract data in the presence of the other. To accomplish this, the designed sequences must be easily distinguished from time shifted versions of itself and each sequence must be distinguished from the other sequence in the set. Every user has an encoder and decoder that is particular to his generated signature coded sequence. The receiver consists of a threshold detector and a pulse generator to reproduce the original stream of data. Each optical component is comprised of a 1x4 splitter and a set of delay lines. The loops on the delay lines signify different lengths.

The output of the laser pulse is optically converted to the prescribed pulse sequence by a parallel fiber-optic line encoder. The line lengths are selected to produce the proper spacing between pulses in the sequence which converts the initial laser pulse into a desired sequence output pulses. When the input optical pulse enters the 1x4 splitter, it splits into four separate output lines. Assuming equal power division (ideal situation), the power of the initial pulse is reduced by one fourth. Each line delays the optical pulse the number of delay units required to satisfy the optical orthogonal code (OOC) requirement. The four pulses are then recombined through the 4x1 splitter. The optical power is again reduced by one fourth. The resultant output is a four-pulse coded sequence with the designed spacing which is characteristic to each user.

The output of the optically coded sequence from the encoder is distributed to each receiver via a 2x2 splitter. This means that each user receives both output coded

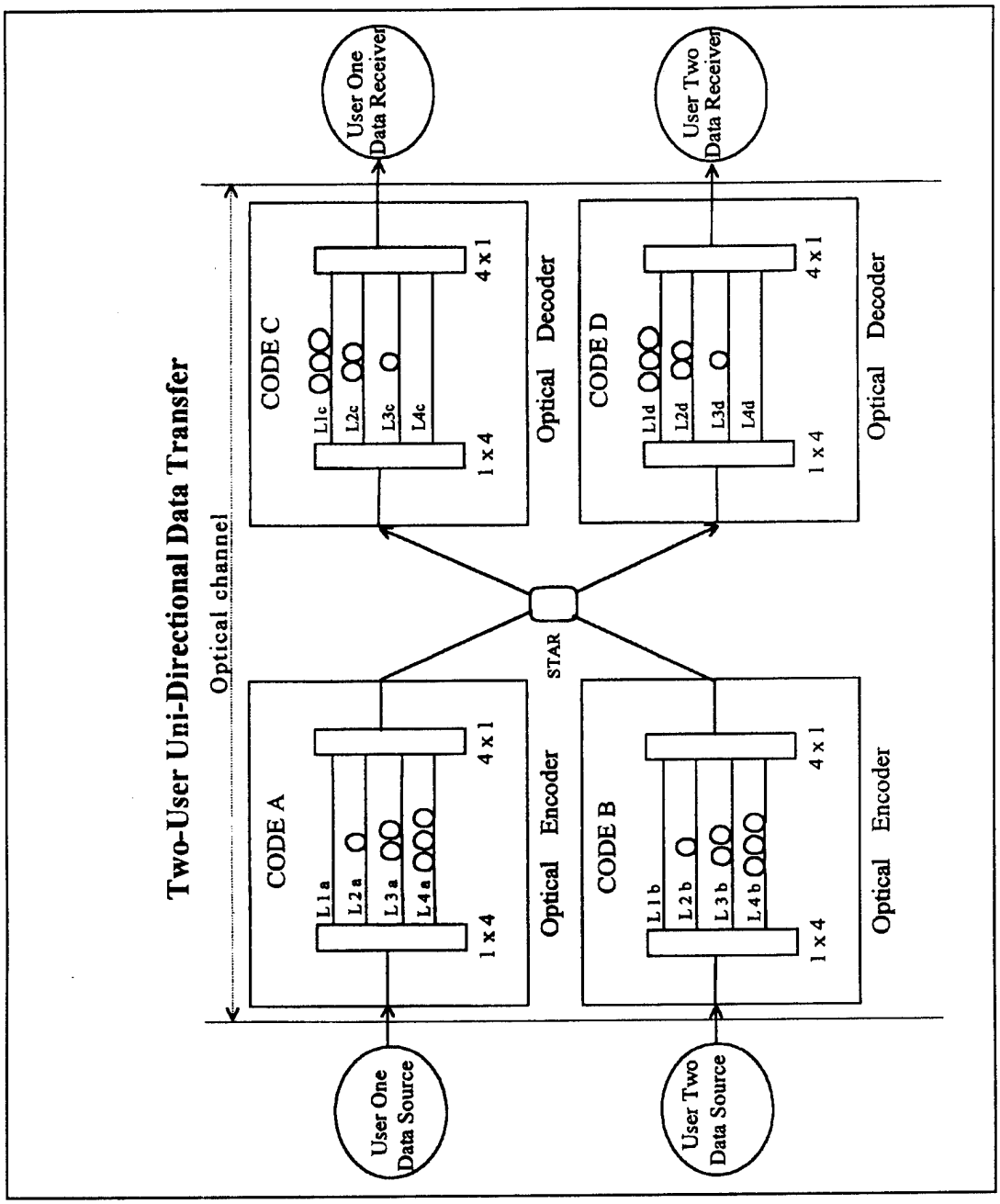

Figure 6. Two-User Optical Fiber CDMA Communication System. [Ref. 6: p. 22]

sequences. The coded sequences used for addressing are designed to produce a high peak correlation when properly matched; otherwise the output is a low peak cross-correlation.

The decoder (correlator) is another set of delay lines which are inversely matched to the encoded pulse spacing. The matched correlator is used to recognize the arrival of the designed sequence. When the optical pulse sequence arrives at the receiver through the encoder, the optical output intensity traces out the correlation function of that sequence. This produces a peak value when the sequence exactly fills the correlator. The correlator effectively integrates the pulses of the sequence. Matched correlation is a term used for auto-correlation which is the similarity between a signal and a time shifted version of itself. Cross-correlation or unmatched correlation is the similarity between a signal and a time shifted version of another signal. In this system of optical orthogonal codes, the auto-correlation is a maximum while the cross-correlation is held to a minimum.

The input to each decoder is a coded sequence from the encoder. The length of the sequence is evenly divided into fourteen unit delay bins. Each line delays the sequence appropriately such that one of the four pulses for each delayed sequence aligns in only one unit delay bin. The power of the coincident pulses are additive and produces a main signal peak that is four times the residual optical power. In this case the "residual optical power" is the power in each individual bin.

The decoders undergo the same type of power loss that occurred in each of the encoders. Each pulse from the encoded sequence is sent through a 1x4 splitter which undergoes coupling and fiber attenuation. The amplitude of the output pulses from the 1x4 splitter is reduced by a factor of four. These pulses are again reduced by the same amount when recombined using the 4x1 splitter. As the sequences pass through the correlator (decoder), their individual intensity is converted to an electrical signal. The signal can now be displayed on an oscilloscope.

The described system demonstrates multiplexing and demultiplexing that is done by optical components, thus exploiting the advantages of a complete optical fiber network. Another consideration of using this technique is that all correlations are done optically,

thereby achieving higher speeds than their electronic counterpart. By using optical orthogonal codes in this system, synchronization between the transmitter and receiver is unnecessary. One last advantage to note is that the system obtains asynchronous communications that is free of network control among many users.

B. CDMA COMPONENTS

Component selection is crucial to the successful implementation of CDMA. In the previous chapter the orthogonal codes were determined for the system to be constructed. This section discusses the highest data rate and hardware for implementation.

1. Bit rate.

Bit rate is defined as [Ref. 4: p. 373]:

$$R_b = 1/T \tag{17}$$

where T_b is the data bit period. The relationship between the laser pulsewidth, T_c, and the data bit period is [Ref. 4: p. 373]:

$$Tc = T_b/ \tag{18}$$

where L is the length of the coded sequence. The length of the coded sequence was shown to be equally divided into fourteen time intervals. If the laser pulsewidth is 5 ns, then it follows that the data rate period is 70 ns. From Eq. 17, the bit rate is 14.29 Mb/s; therefore the pulse code generator selected must have a data rate at least equal to or less than this value.

2. Source

The source used for this thesis is a high speed optical laser transmitter with a maximum modulation rate of 1.2 Gb/s. The wavelength for the device is 1300 nm. There are many benefits to using this laser as a source. In the short wavelength region, the dispersion characteristic in silica fiber and spectral linewidth limits the data-rate-distance product to approximately 150 (Mb/s)km [Ref. 6: p. 26]. Using a wavelength at 1300 nm causes lower attenuation and dispersion within the optical fiber. The optical output pulse rise-fall time of 0.5 ns tends to produce a sharp square waveform. This helps to create accurate pulse positioning in the coded sequence.

3. Detector

The detector that was used was a wideband, high speed optical to electrical (O/E) converter in conjunction with a 26 dB linear amplifier. The device utilizes a high speed

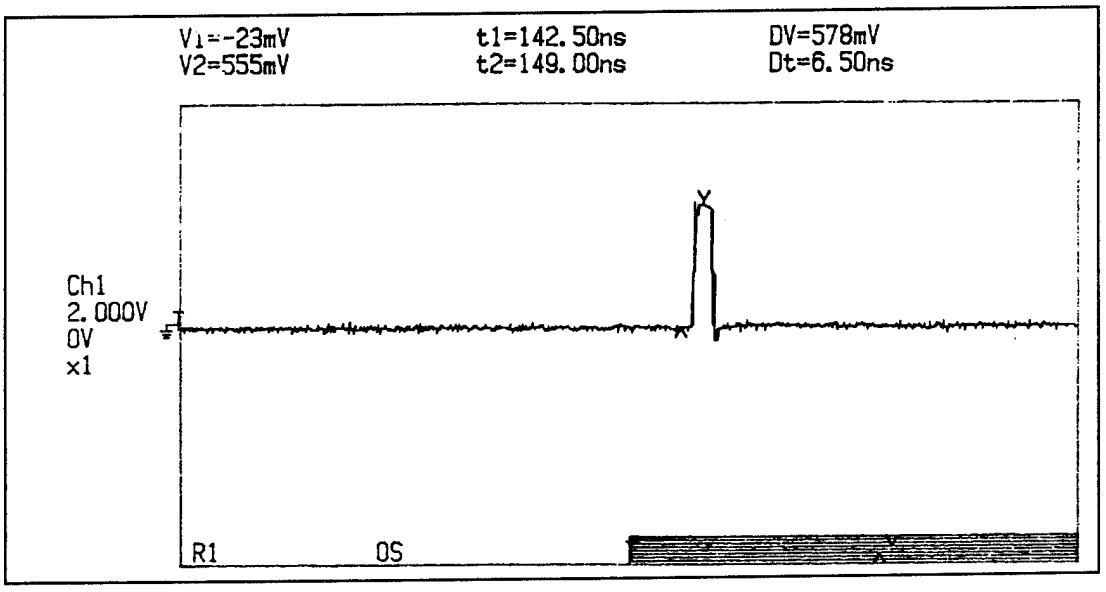

Figure 7. Waveform from Laser Source.

Germanium avalanche photodetector diode (APD), which allows optical waveforms from less than 100 nW to more than 100 μW to be accurately reproduced. Appendix A depicts a conversion chart of the average optical power (dBm) to the minimum output signal (mV), for the particular detector. Figure 7 shows the output waveform from the laser to the detector which is displayed on the oscilloscope. In this and preceding figures, two cursors are used to express the maximum and minimum output levels of each signal. The first cursor is designated as "v" its voltage level (v1) and position (t1) which is displayed in the upper margin. The second cursor denoted as an inverted "v", displays the voltage level (v2), and position (t2), beneath the cursor one's output.

4. Pattern Generator

To generate the necessary bit pattern, a Hewlett Packard Error Performance Analyzer and Pattern Generator model were used [Ref. 10: p. 45]. This equipment produces and analyzes patterns with data rates from 36 bit/sec up to 1 Gbit/s. The pattern generator output is a NRZ binary data and has the option of producing a complement of the data, clock signal, compliment of the clock signal and a trigger pulse. It allows the operator to inject external errors to perform bit error analyses. The user-determined patterns are generated as parallel pattern generator sequences. Each rising edge is performed at TTL levels.

The error detector module accepts in-coming NRZ binary data and a clock signal via the first panel DATA IN and CLOCK IN ports. It then performs various comparisons and measurements on the data stream to determine the error count and the error rate of relative to its stored reference patterns. The error output and trigger output allows the operator to view the error occurrences on an oscilloscope.

A clock signal at the incoming data rate is an input via the CLOCK IN port. The signal out is fed to a vernier hybrid which introduces a variable delay into the clock signal path. This time delay has a resolution of 1 ps. The phase shifter gives a time shift in the relative positions of the clock and data edge of ± 1 ns.

In PATTERN mode, the trigger pattern that the user enters is matched to the pattern being generated and a trigger pulse is the output when the two correspond. In this thesis a pattern generator length of 64 bits was selected with a single one in the pattern. Later as the communication system was working properly, the signal was made more complicated.

The clock frequency sets the gating period of the selected pattern. A clock frequency of 200 MHz was selected to produce a square wave pulse with a 5 ns pulsewidth.

This equipment provided (with great accuracy), the necessary bit patterns to generate the coded sequences. Once the codes were generated and passed through a threshold detector, the resultant was sent through the error analysis and produced an error count of zero.

5. Oscilloscope

The selected oscilloscope was a Tektronix RTD 720A model Transient Digitizer. This is a high bandwidth, fast sample rate, long record length digitizer designed to accurately capture fast transient events [Ref. 11: p. 30]. A single analog signal path is maintained even at the highest acquisition rates for high performance operation in all vertical operating modes. It has a full bandwidth of 500 MHz with sampling rates at 26 S/s to 5 MS/s. The sample rate interval determines the highest frequency signal component that can be recorded. This is called the Nyquist frequency and is equal to sample rate divided by two. The sample interval multiplied by the record length equals duration of the acquisition window. A sample interval of 1 ns, a rate of 1 GS/s and an acquisition record length of 512 points were the parameters for the recorded measurements.

The display above the waveform picture is referred as the cursor readout. The displayed cursor information is absolute time, voltage for each cursor amplitude between each cursor (ΔV) and the time between cursor (Δt). The cursors are identified as "$\vee$", (cursor 1) and "$\wedge$" (cursor 2). Figure 7 is a typical output of the Tektronix Digitizer .

6. Fiber

This thesis utilized 50 μm multimode fiber for ease of splicing, adding connectors, and coupling laser power.

7. Power Budget

From Figure 6 it is easy to see the large amount of couplers, optic lines and optical splitters used in the construction of this system. The numerous variables that go into power loss accountability such as coupling misalignments and splitting losses, makes the construction of this network extremely difficult.

This problem can be simplified by utilizing vector notation. Each sequence contains pulses in four of the fourteen unit delay bins; therefore, there exists only four nonzero entries in a vector representing the coded sequence.

In the encoder, the initial pulse is split into four pulses by the 1x4 splitter (which undergoes a power loss of -8 dB) and is represented in vector form as l = [-8 -8 -8 -8]. The signal is attenuated by each delay line of -1 dB. Each successive loss is added to give a cumulative loss of l = [-9 -9 -9 -9]. The output of the delay lines are combined in a 4x1 splitter which again gives a loss of -8 dB; therefore, the total output from each encoder becomes l =[-17 -17 -17 -17]. The output of the encoder is sent through a 2x2 splitter which contributes a loss of -1.5 dB, making the vector representation of each decoder input l = [-18.5 -18.5 -18.5 -18.5].

An important concept to realize is that a single pulse enters the encoders producing a sequence which can be represented as a vector. Each sequence is appropriately delayed as they travel through the decoders, thus producing a correlation at the output. This correlation can be represented as a matrix. The first 1x4 splitter induces a -8 dB loss thereby producing four delayed sequences in matrix form as

$$I = \begin{bmatrix} -26.5 & -26.5 & -26.5 & -26.5 \\ -26.5 & -26.5 & -26.5 & -26.5 \\ -26.5 & -26.5 & -26.5 & -26.5 \\ -26.5 & -26.5 & -26.5 & -26.5 \end{bmatrix}. \tag{19}$$

Here each row represents one of the delayed sequences. The sequences are sent through each corresponding delay line (-1 dB) and are summed with the final 4x1 splitter (-8 dB) which gives the total attenuation in the system as

$$I = \begin{bmatrix} -35.5 & -35.5 & -35.5 & -35.5 \\ -35.5 & -35.5 & -35.5 & -35.5 \\ -35.5 & -35.5 & -35.5 & -35.5 \\ -35.5 & -35.5 & -35.5 & -35.5 \end{bmatrix}. \tag{20}$$

The delay lines of the encoder are constructed such that one of the four pulses in each coded sequence aligns in only one unit delay bin. This means the optical power of each of the four sequences are coincident at the output. The first pulse of each sequence that experiences the longest delay arrives at the output of the decoder, while the last pulse experiences the shortest delay. If the first and last rows of the matrix I represents the fastest and slowest sequence, respectively, then the coincident pulse are on the left diagonal of matrix I [Ref. 2: p. 34]. Utilizing the concept of auto-correlation, the summation of the optical power contained in these four pulses produces a pulse with an optical power level four times greater (+ 6 dB) than the individual pulses. The remaining pulses are noncoincidental and therefore produce a residual power output.

The effect of auto-correlation produces a waveform with a single main signal peak at the output. The losses incurred at the output of the decoder is represented as

$$I = [x, x, x, x, x, x, y, x, x, x, x, x, x] \tag{21}$$

where x is equal to -36.5 dBm and y is equal to -29.5 dBm. This sequence represents the auto-correlation which consists of a main signal peak (y) that is four times the residual power (x). Due to the numerous splitters, couplers and fiber attenuation, the power loss of a CDMA system is quite severe. However, the requirement in selecting optical orthogonal codes are that the signal must be distinguished from time shifted versions of itself and it must be distinguished in the presence of other coded sequences. Both these requirements are satisfied in Eq. 21. The auto-correlation produces a peak that is four times the residual power output.

Figure 6 shows a detailed schematic of the CDMA system designed in a star configuration that implements (0,1) pulse sequences by sets of parallel fiber-optic delay lines. The produced sequences are distinguishable from the other sequences in the set. This chapter described each component that was utilized in the design of the CDMA system. The proceeding chapter construes in more detail the construction of the encoders and decoders that utilizes the optical orthogonal coded sequences.

IV. ENCODERS

A. DESIGN

The selection of a suitable pulse sequence is the major concern in code design. The set of optimal sequences that posses both minimal levels of pairwise cross-correlations and minimal levels of off-peak auto-correlation are designed as pseudo-orthogonal codes. The minimum sequence length for a two user system is 14 with a code weight of 4 [Ref. 8: p. 22]. The code "weight" refers to the number of pulses. The placement of theses pulses are multiples of the chip interval delay which is determined by the length of the fiber. The solution for the pseudo-orthogonal code set is generated by a computer. A code with the proper placement is shown in Table 2.

Table 2. Graphical Representation of Coded Sequences.

g(2,4)														
X	1	0	0	1	0	0	0	0	0	0	0	0	1	1
delay units	0			3		5		7				11	12	13
Y	1	0	0	0	0	1	0	1	0	0	0	1	0	0

To place the pulses in the correct position the delay time must be calculated from the fiber length. The speed of light in an optical fiber, v, is determined by the ratio of the velocity of light in a vacuum and the index of refraction, n.

$$v = \frac{c}{n} = \frac{3 \times 10^8}{1.47} = 2.04 \times 10^8 \; m/s. \tag{22}$$

A pulse width of 5 ns was used as the unit delay time in this thesis. To determine the length of the optical fiber delay line, the speed of light in the optical fiber is multiplied by the unit delay time to give

$$d = v \cdot t = (2.04 \times 10^8 m/s)(5 \times 10^{-9} s) = 1.0197\ m. \quad (23)$$

The following are the calculated delay lengths for the various position of the sequence used.

Table 3. Delay Line Lengths.

Chip time = 5.00E-9	
Delay required	Length in meters
0	0
1	1.02
2	2.04
3	3.06
4	4.08
5	5.1
6	6.12
7	7.14
8	8.16
9	9.18
10	10.2
11	11.22
12	12.24
13	13.26

Table 4 is the calculated lengths of the delay lines required to place the pulses in the proper position to implement the sequence code. This is a quick summary of Table 3

for the positions of interest. The length for the first pulse in both the X and Y sequence is equal to zero signifying that no delay is required.

Table 4. Encoder Delay Line Lengths.

g(2,4)	Sequence X	Sequence Y
Pulse no.	Length in meters	Length in meters
1	0	0
2	3.06	5.11
3	12.24	7.14
4	13.26	11.22

B. CONSTRUCTION

The construction of the encoder requires a 1x4 splitter, three delay lines, a 4x1 splitter and 18 ST-style connectors. If uniform splitting and connector losses are assumed, the construction is trivial. However, in reality, these components do not possess uniform losses and the construction becomes a difficult problem in power loss management.

The design of the encoder must produce a sequence of uniform amplitudes at the output. This requires connecting the components in a particular combination such that amplitudes of the delayed output are approximately uniform.

To show how difficult this problem is, consider the typical losses in each component. The 1x4 splitters exhibit losses ranging from -5.5 dB to -11.0 dB. The mechanical connectors may insert losses as high as -2.0 dBm. The delay lines insert losses ranging from -0.5 dB to -1.9 dB. To complicate this problem even further, the components do not exhibit symmetric bi-directional losses. The power loss of each component depends on the placement of the source and detector. This is not so much a problem for the delay lines but it is a critical issue for the splitters. Even though the 1x4 splitter is the same device as the 4x1 splitter, the measured losses are dramatically

different. For example, while the 1x4 splitter may insert a loss of -6.0 dB, the 4x1 splitter can insert a -8.0 dB loss. Ideally we would expect the same loss to occur no matter how it was measured. However, during the construction of the splitters the diameters of the fibers are not aligned perfectly. Thus, the measured values depends on the direction of the pulse.

The power loss of all components were found experimentally by an insertion loss approach. This approach requires the components to be connected to a known power source at the input while the losses are measured by a power meter at the output. The delay lines were constructed so that the maximum insertion loss is -2.0 dBm. The connectors were repolished until the losses were less than the maximum allowable loss.

The attenuation specification for the fiber used in this thesis was -2.8 dB/km; therefore, it is clear that the bulk of the insertion loss is caused by the connectors.

Appendix B contains the measured results for all eight 1x4 and 4x1 splitters. Each device has the option to act as a 4x1 or 1x4 splitter; therefore, the appendix shows sixteen different combinations.

To achieve uniform amplitude for the output pulses, the right combination must be selected from the tabulated results. Each decoder must have a 1x4 and 4x1 splitter for each set of given delay lines. The problem then is to select the proper splitters for each set of lines.

Appendix C is a MATLAB program written by J.W. Andre [6] that was used to optimize the selection of each combination. The measured losses of each splitter are placed in a matrix. The measured losses for the delay lines are placed in a row vector *b*. The program assigns unequal row vectors to variables *r*1 and *r*2. The three vectors (*b*, *r*1 and *r*2) are added and the standard deviation is taken from the sum. If the standard deviation is less than the previous stored value, the three vectors are stored for the output. The vectors are rotated right four times (similar to a circular buffer operation), one at a time, and a new sum is computed. The standard deviation is taken and compared. The process continues for all vectors in the matrix. In essence the computer generates all

possible combinations to calculate a solution that is less than the selected standard of deviation. In this case the final standard of deviation was 2.0 [Ref. 6: p. 40].

Once the optimum combination is determined for a set of delay lines, the corresponding data for the selected splitters are removed from the data matrix. This process is carried out for the next set of delay lines. The standard of deviation for each splitter combination range from 0.4 to 1.8, thus proving to be a very efficient way of determining the proper combination. The results for the two sets of encoders are tabulated in Table 5.

Table 5. Encoder's Order of Assembly.

Encoder Y	Measured losses (dB)			
580A	-8.7	-8.9	-8.1	-8.2
586B	-8.1	-7.7	-8.6	-9.1
Delay line losses	-0.4	-0.5	-0.7	0
Sum of losses	-17.2	-17.1	-17.4	-17.3
Encoder X	Mesured losses (dB)			
585A	-8.3	-6.9	-7.1	-9.5
581B	-8.4	-8.6	-8.1	-6.8
Delay line losses	0	-1.2	-1.2	-1.1
Sum of losses	-16.7	-16.7	-16.4	-16.4

C. PERFORMANCE

The outputs of the X and Y encoder are shown in Figures 8 and 9, respectively. For each output a band diagram is placed under the coded waveform. This band diagram contains the predicted fourteen-segment output code, where each interval is 5 ns long. The projected positions of the pulses are shaded. From these diagrams it is clear that the projected pulse positions matches with the actual output for both the X and Y sequences.

The amplitude of the output pulses for the X sequence are nearly equal. The highest detected peak is 578 mV while the lowest is 570 mV, thus producing a deviation of 8 mV. Using Appendix A, the input power levels should be approximately -21.4 dBm and -21.5 dBm.

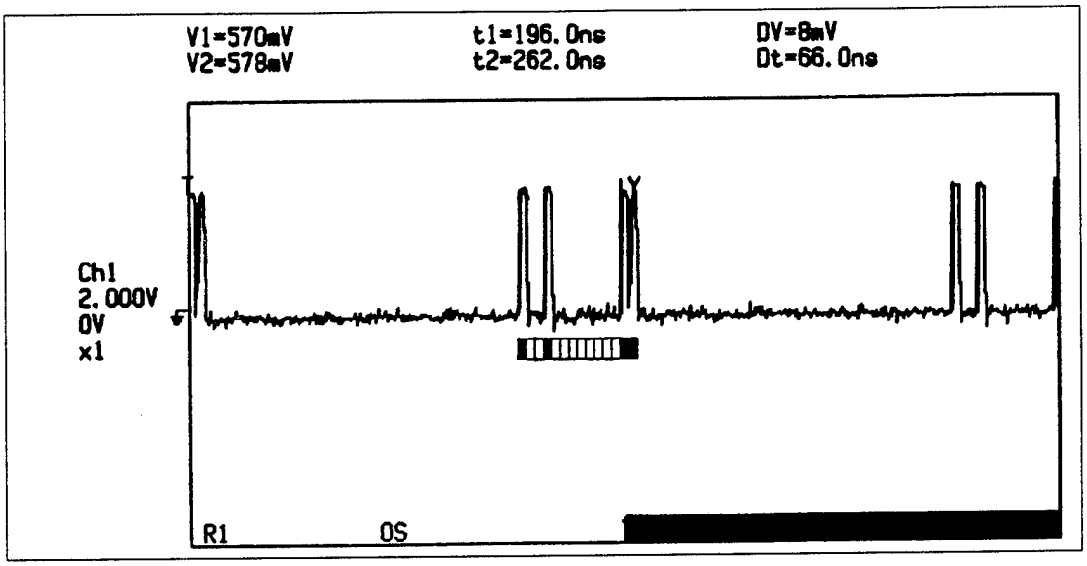

Figure 8. Sequence X.

From Table 5 the lowest loss for the X encoder is -16.4 dBm; when combined with the measured initial loss of -4.5 dBm, the total is -20.9 dBm. Using Appendix A, the voltage output from the detector is 48 mV. This is increased by using a 26 dB amplifier; therefore, the final output becomes 624 mV. The highest loss from Table 5 is -16.7 dBm. When combined with the initial loss, the total loss becomes -21.2 dBm. Using Appendix A, the output of the detector is 44 mV. The output from the amplifier is then 572 mV. These values are near the observed voltage levels.

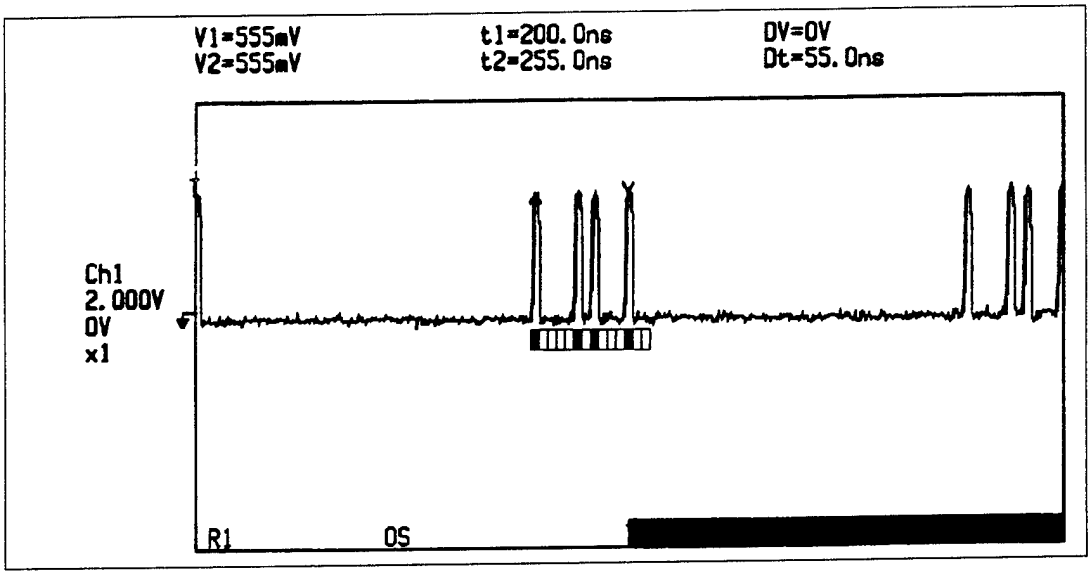

Figure 9. Sequence Y.

Taking a look at the Y sequence, the highest peak is 594 mV, while the lowest is 563 mV. From Appendix A, the input power levels should be approximately -21.0 dBm and -21.5 dBm. The deviation in this case is 31 mV or -0.5 dBm.

The lowest loss for the Y encoder in Table 5 is -17.1 dBm. When added to the initial loss, the total becomes -21.6 dBm, which corresponds to a detector output of 43 mV. The output from the amplifier is 559 mV. The highest loss in Table 5 is -17.4 dBm resulting in a total loss of -21.9 dBm. This corresponds to a detector voltage of 42 mV and ultimately an amplifier output of 546 mV.

The conclusion from this analysis is that the output voltage levels can be predicted from the measured power loss in each encoder. The predicted voltage output are well within 10% of the observed values and, in many cases, are within 1%.

The pulse amplitudes for the X sequence varies only 8 mV while the Y sequence are equal. The coded output waveforms matched the corresponding components with outstanding results. Even though the components possess unequal power loss, it is possible to construct encoders that produce a coded sequence of near equal amplitudes.

Once the orthogonal code is determined, it is relatively easy to construct the encoders from the calculated delay lines. These delay lines provide the proper spacing between pulses in the sequence. For every pulse that enters the encoder, a sequence exits. Figures 8 and 9 shows the encoders are performing properly. The output is the expected uniform pulse sequence waveform. With the encoders working properly, the next step is to construct the decoders to recover the original data.

V. DECODERS

A. DESIGN

The constructed encoder was a parallel fiber-optic delay line system. The delay lines produce the proper spacing between pulses in the coded sequence. The decoder, therefore, was another set of delay lines that are inversely matched to the pulse spacing. The matched filter must be a reverse replica of the input signal. The graphical representation for the impulse response of the two matched filters can be seen in Table 6.

Table 6. Graphical Representation of Matched Filters.

g(2,4)														
$\underline{X}^{-1}$	1	1	0	0	0	0	0	0	0	0	1	0	0	1
delay units	0	1			4		6				10	11		13
$\underline{Y}^{-1}$	1	0	0	0	1	0	1	0	0	0	0	1	0	0

The lengths of the delay lines were computed from the number of delay units corresponding to the pulse position. From the above table the pulse positions are located at (0,1,4,6,10,11 and 13). The delay time is found by multiplying the number of delay units by the length of one delay unit, *d*. Table 7 shows the calculated delay lengths corresponding to the pulse position for both decoders.

Table 7 is the calculated lengths of the delay lines required to place the pulses in the proper position. This is a quick summary of Table 3 for the positions of interest. The first pulse in both the $\underline{X}^{-1}$ and $\underline{Y}^{-1}$ sequence is equal to zero, signifying that no delay is required.

Once the optimum combination of optical components determined for a given set of delay lines (MATLAB program from chapter 4), the corresponding parts are connected to form the decoder. The standard deviations for each splitter combination range from 0.4

to 1.8, thus proving to be a very efficient way of determining the proper combination. The results for the two sets of decoders are tabulated in Table 8.

Table 7. Decoder Delay Line Lengths.

g(2,4)	Sequence $\underline{X}^{-1}$	Sequence $\underline{Y}^{-1}$
Pulse no.	Length in meters	Length in meters
1	0	0
2	1.02	4.08
3	10.2	6.12
4	13.26	11.22

Table 8. Decoder's Order of Assembly.

Decoder $\underline{X}^{-1}$	Measured losses (dB)			
583A	-7.1	-8.4	-7.3	-9.2
587B	-8.2	-8.2	-8.9	-8.7
Delay line losses	-1.9	-1.1	-1.6	0
Sum of losses	-17.2	-17.7	-17.8	-17.9
Decoder $\underline{Y}^{-1}$	Mesured losses (dB)			
614B	-8.1	-9.1	-9.1	-7.7
584A	-8.1	-7.5	-8.1	-7.5
Delay line losses	-1.2	-0.7	0	-1.9
Sum of losses	-17.4	-17.3	-17.2	-17.1

B. CONSTRUCTION

The decoders were tested by sending a single pulse with a pulse width of 5 ns and recording the output waveform. As expected the single pulse produces four pulses. The results of the $\underline{X}^{-1}$ and $\underline{Y}^{-1}$ decoders are shown in Figures 10 and 11, respectively. A band diagram is placed underneath each waveform. Each segment represents 5 ns in time and the predicted pulse positions are shaded. It is clear that these pulses align with the band diagram and, therefore, occur in the correct position. By comparison, the $\underline{X}^{-1}$ and $\underline{Y}^{-1}$ decoders are the reverse conjugate of the $\underline{X}$ and $\underline{Y}$ encoders.

The amplitude of the output pulses for the $\underline{X}^{-1}$ sequence are nearly equal. The $\underline{X}^{-1}$ decoder reveals that the highest peak has a receiver voltage of 555 mV while the lowest is 547 mV. The result is a deviation of only 8 mV or 1.4%.

From Table 8, the lowest loss is -17.2 dBm and, when combined with the measured initial loss of -4.5 dBm, the total loss is -21.7 dBm. Using the chart in Appendix A, the predicted output voltage from the detector is 43 mV. The output is then increased by a 26-dB amplifier, resulting in a voltage output peak of 559 mv. The highest loss from Table 8 is -17.9 dBm and, when added to the initial loss, the total becomes -22.4 dBm. From Appendix A, the predicted detector's output is 42 mV and, in conjunction with the amplifier, the result is a peak output voltage of 546 mV. These results are in complete agreement of the measured values of 555 mV and 547 mV.

Analyzing the $\underline{Y}^{-1}$ decoder, the highest output is 594 mV while the lowest is 563 mV. Though the deviation is greater for this decoder, the peak amplitudes are still nearly equal. The deviation for this decoder is 31 mV or 5.2%.

From Table 8, the lowest loss for the $\underline{Y}^{-1}$ sequence is -17 dBm. When combined with the initial loss (-4.5 dBm), the total loss becomes -21.5 dBm. Using the detector gain chart, the voltage output is 44 mV; therefore, the resultant from the amplifier is a peak of 572 mV. The highest loss from Table 8 is -17.4 dBm which corresponds to a final output voltage of 559 mV.

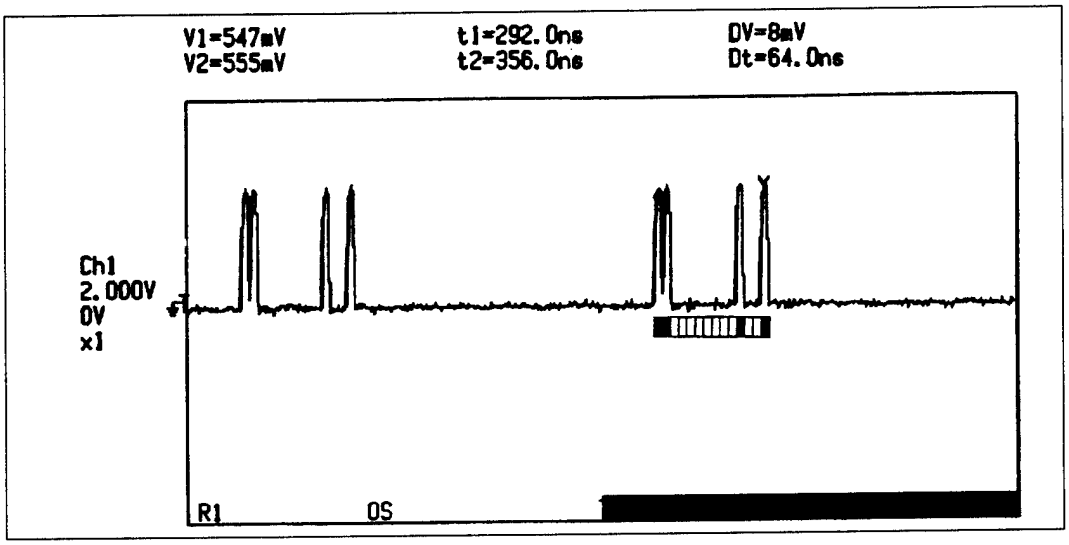

Figure 10. Impulse Response For Sequence $\underline{X}^{-1}$

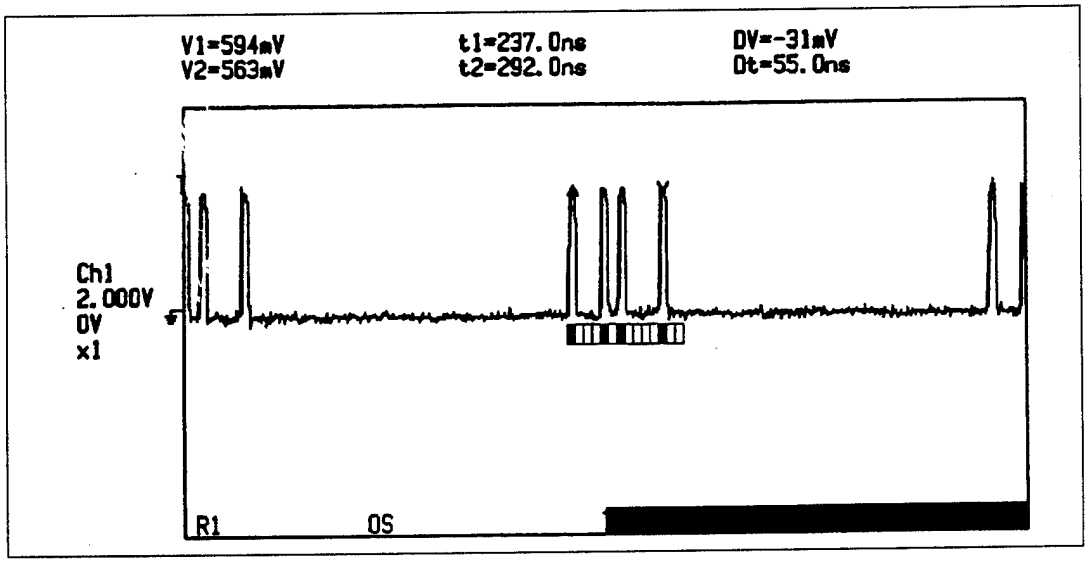

Figure 11. Impulse Response For Sequence $\underline{Y}^{-1}$

The observed peak output voltage agrees with calculated output. The output voltage can be predicted with good accuracy by measuring the optical power loss from the components of the decoder.

The decoder is a set of delay lines that are inversely matched to the encoders. For every pulse that enters the decoder, a sequence of four pulses exits. Figures 10 and 11 shows the decoders to be operating properly. A single pulse was injected into the decoders and the proper sequence emerges. Comparing the output from the encoders to the decoders, it is easy to see they are mirror images of each other. Now that the encoders and decoders are performing perfectly, the next step is to cascade the components to perform the correlation functions.

VI. RESULTS

A. AUTO-CORRELATION

The previous chapters illustrated the construction of the encoders and decoders. The separate devices were tested and proven to be operating properly. In this section the encoders and decoders are connected by a 2x2 splitter and the combined output is recorded.

The purpose in using a set of orthogonal coded sequences was to maximize the auto-correlation and to minimize the cross-correlation. This can be better seen by graphical representation. Table 9 shows the auto-correlation for the $\underline{X}$ sequence. The sequence is shifted in time corresponding to the decoder time delay. The decoder delays occur at (0,1,10 and 13); therefore, the coded input is shifted in time at four different positions. The first position, 0, is without delay. The four coded sequences are added to give an output sequence which has a main peak located at the center with an amplitude four times that of the others.

One of the properties of orthogonal codes is that the auto-correlation produces an output signal with a main signal peak equal to the residual power multiplied by the code weight. (The code "weight" is the number of pulses in the encoded sequence. In this case, the code "weight" is four). The residual power output is the output due to the power loss from the combined components.

Figure 13 shows the experimental output waveform for the auto-correlation of the $\underline{X}$ sequence. Again a band diagram is placed underneath the observed waveform as a quick reference for the predicted output. The fully shaded segment represents the main signal pulse while the half shaded segments corresponds to the residual pulses. Combining the losses from the $\underline{X}$ encoder, the $\underline{X}^{-1}$ decoder and the 2x2 splitter (-1.5 dBm), the total is -37.6 dBm. Using Appendix A, the detector's output is predicted to be 3.7 mV. The residual voltage output from the amplifier is 48.1 mV. The main signal pulse is then 192.4 mV (four times the residual). The observed residual voltage peak is 59 mV while the main

signal peak is 201 mV. These values are extremely close to the expected output. The maximum is quite close to four times the residual, confirming a properly functioning system.

The same process is used to analyze the $\underline{Y}$ auto-correlation. The graphical representation for the $\underline{Y}$ sequence is shown in Table 10. The encoded sequence is shifted in time by the time delay sequence of the decoder. Because of the nature of the orthogonal code, the correlation produces a sequence with a maximum peak four times the residual. Figure 15 shows the observed output with the band diagram.

The predicted output is derived by summing losses of the $\underline{Y}$ components (-33.6 dBm), the initial loss (-4.5 dBm) and the 2x2 splitter (-1.5 dBm). The total loss is -39.6 dBm. From Appendix A, the residual voltage level is 36.4 mV, which corresponds to a main signal voltage peak of 145.6 mV. The observed output shows the maximum peak at 145 mV while the residual is 41 mV. This data confirms the correct operation of the auto-correlation of the Y sequence.

B. CROSS-CORRELATION

Table 11 shows the graphical representation for the cross-correlation of the $\underline{X}$ and $\underline{Y}^{-1}$ sequence. The coded input $\underline{X}$ sequence is shifted in time by the $\underline{Y}^{-1}$ decoder. This time, however, there is no alignment for a main signal peak. The total loss sent through the $\underline{X}$ and $\underline{Y}^{-1}$ devices is -39.6 dBm. Using Appendix A, the output should be 36.4 mV.

Figure 17 is the observed cross-correlation with the band diagram of the predicted output. The predicted waveform matches the observed output. Also, the observed output amplitude is 33 mV which is very close to the prediction from the power loss. This data confirms the correct operation of the cross-correlation of $\underline{X}$ and Y^{-1}.

Table 12 is the graphical representation of the $\underline{Y}$ and $\underline{X}^{-1}$ sequence. Using the same analysis as in the $\underline{X}$ and $\underline{Y}^{-1}$ sequence, there is no main signal peak. The total loss is -39.4 dBm corresponding to a 38.5 mV output.

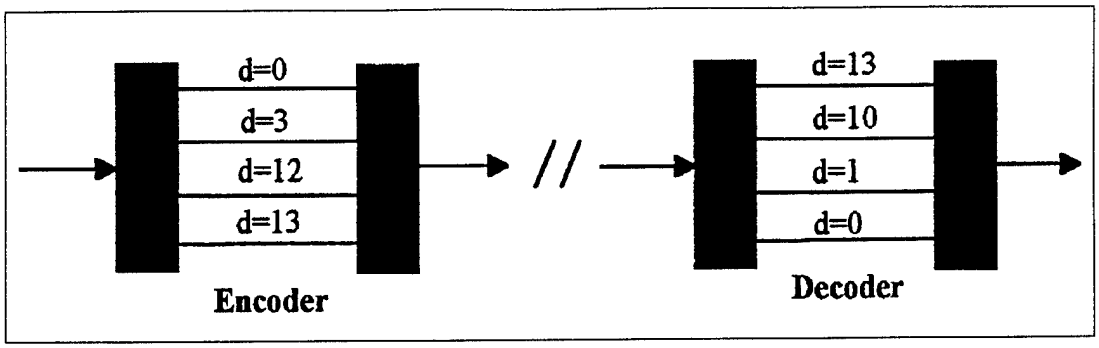

Figure 12. Encoder and Decoder Delays for Sequence X.

Table 9. Auto-Correlation of Sequence X.

1	0	0	1	0	0	0	0	0	0	0	0	1	1															
1	0	0	1	0	0	0	0	0	0	0	0	1	1															
	1	0	0	1	0	0	0	0	0	0	0	0	1	1														
										1	0	0	1	0	0	0	0	0	0	0	0	1	1					
													1	0	0	1	0	0	0	0	0	0	0	0	1	1		
1	1	0	1	1	0	0	0	0	0	1	0	1	4	1	0	1	0	0	0	0	0	1	1	0	1	1		

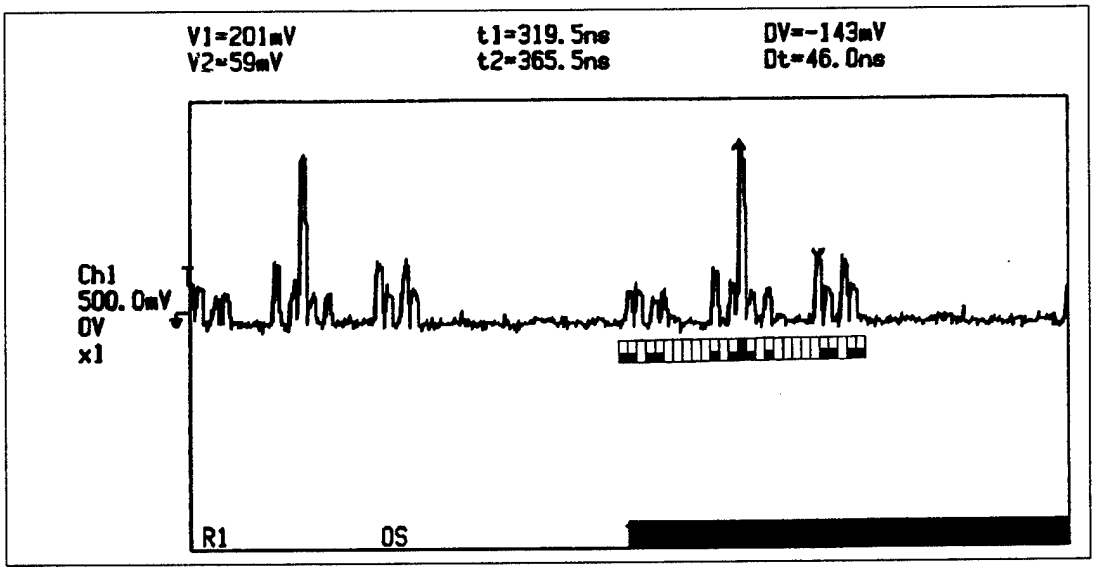

Figure 13. Auto-Correlation Waveform for Sequence X.

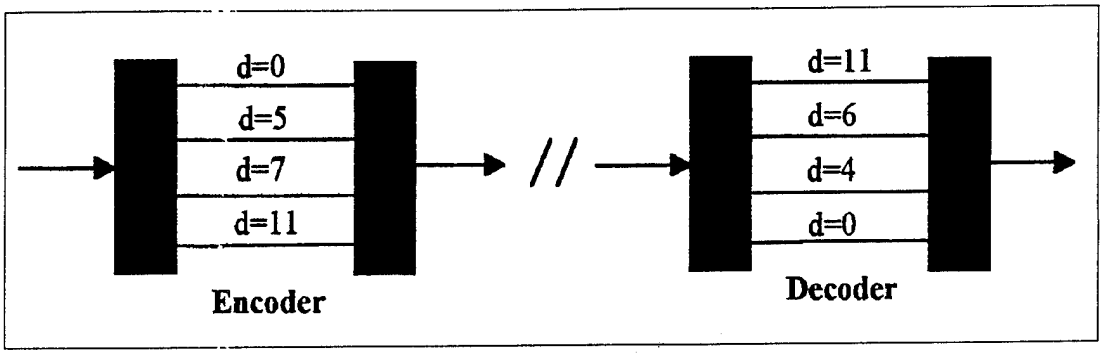

Figure 14. Encoder and Decoder Delays for Sequence Y.

Table 10. Auto-Correlation of Sequence Y.

1	0	0	0	0	1	0	1	0	0	0	1	0	0															
1	0	0	0	0	1	0	1	0	0	0	1	0	0															
		1	0	0	0	0	1	0	1	0	0	0	1	0	0													
				1	0	0	0	0	1	0	1	0	0	0	1	0	0											
									1	0	0	0	0	1	0	1	0	0	0	1	0	0						
1	0	0	0	1	1	1	1	0	1	0	4	0	1	0	1	1	1	1	0	0	0	1	0	0				

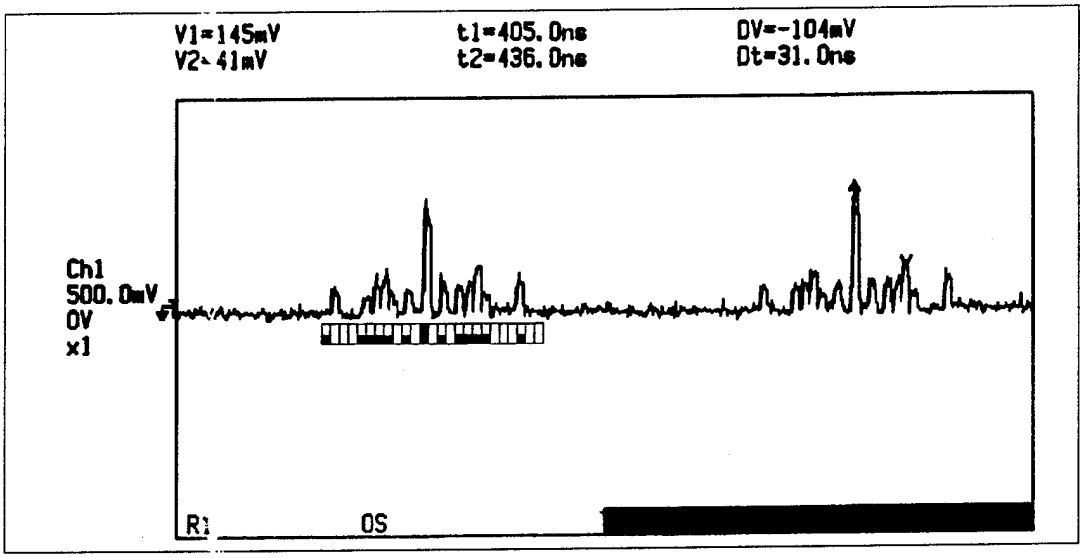

Figure 15. Auto-Correlation Waveform for Sequence X.

Figure 19 is the observed output with the band diagram of its predicted output. The corresponding peaks align very nicely. The observed voltage output is 53 mV which is near the expected 38.5 mV. Taking into account that 53 mV is the maximum while 29 mV is the minimum, the data is quite good. This again confirms the correct operation of the $\underline{Y}$ and $\underline{X}^{-1}$ cross-correlation.

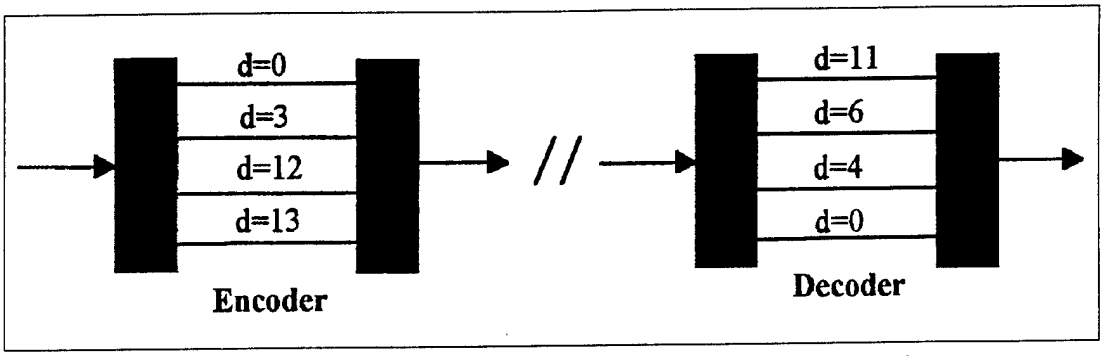

Figure 16. Encoder and Decoder Delays for Sequence $\underline{X}$ and $\underline{Y}^{-1}$.

Table 11. Cross-Correlation of Sequence $\underline{X}$ and $\underline{Y}^{-1}$.

1	0	0	1	0	0	0	0	0	0	0	0	1	1													
1	0	0	1	0	0	0	0	0	0	0	0	1	1													
			1	0	0	1	0	0	0	0	0	0	0	0	1	1										
						1	0	0	1	0	0	0	0	0	0	0	1	1								
									1	0	0	1	0	0	0	0	0	0	0	0	0	1	1			
1	0	0	1	1	0	1	1	0	1	0	1	1	1	1	0	1	1	1	1	0	0	0	1	1		

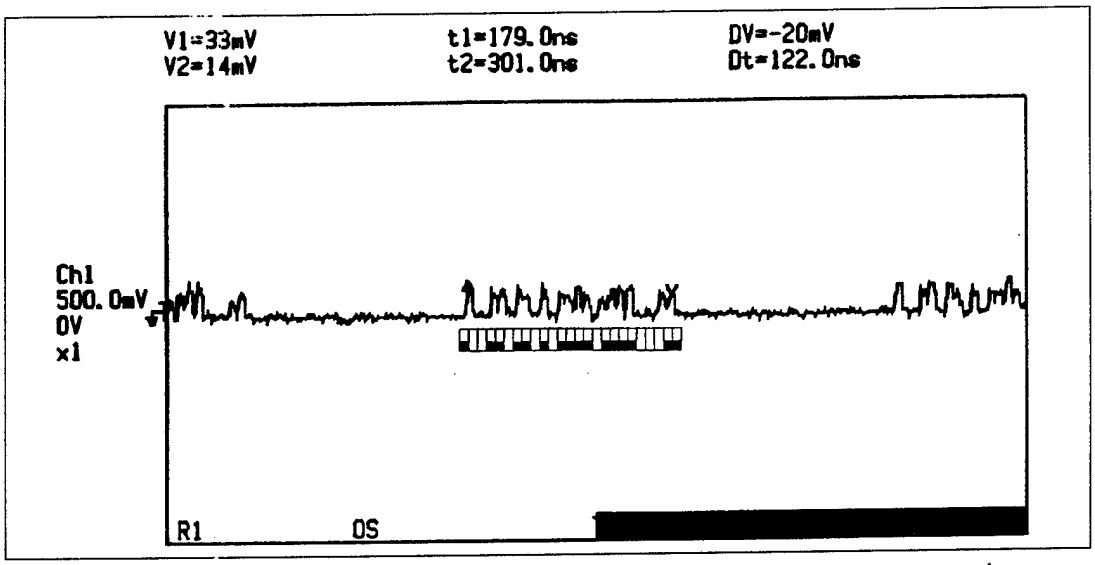

Figure 17. Cross-Correlation Waveform for Sequence $\underline{X}$ and $\underline{Y}^{-1}$.

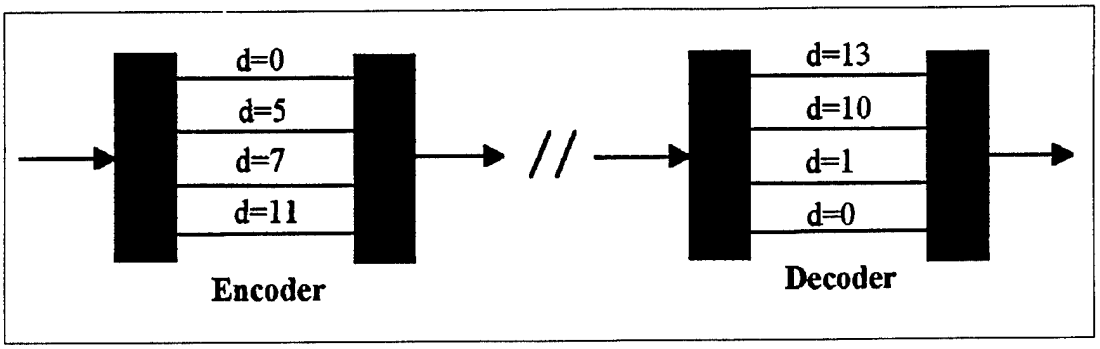

Figure 18. Encoder and Decoder Delays for Sequence $\underline{Y}$ and $\underline{X}^{-1}$.

Table 12. Cross-Correlation of Sequence $\underline{Y}$ AND $\underline{X}^{-1}$.

1	0	0	0	0	1	0	1	0	0	0	1	0	0	
1	0	0	0	0	1	0	1	0	0	0	1	0	0	
	1	0	0	0	0	1	0	1	0	0	0	1	0	0
				1	0	0	0	1	0	1	0	0	0	1	0	0
							1	0	0	0	1	0	1	0	0	0	1	0	0
1	1	0	0	0	1	1	1	1	0	1	1	1	1	1	0	1	1	0	1	1	0	0	1	0	0

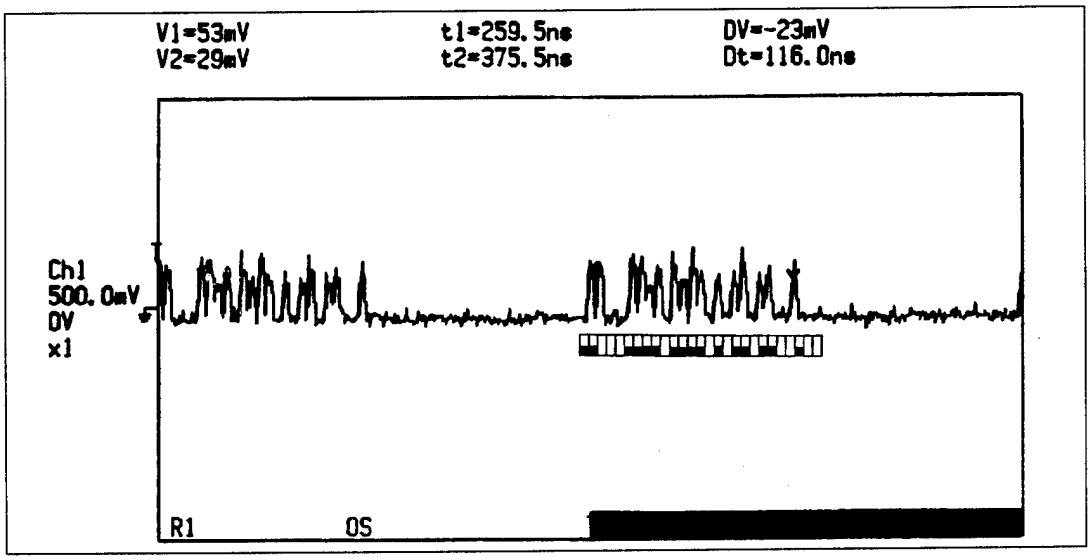

Figure 19. Cross-Correlation Waveform for Sequence $\underline{Y}$ And $\underline{X}^{-1}$.

C. SIMULTANEOUS OPERATION

The last section demonstrated that the encoder/decoder combinations were functioning properly. This in its self is not enough. For a successful operation, both encoders must operate simultaneously. This section analyzes simultaneous operation of the devices.

The goal of CDMA is to provide asynchronous access to each user and permit simultaneous access with no waiting time. For simplification the input signal to each encoder is confined to a single pulse. The input to the $\underline{X}$ encoder was subjected to a variable delay to the show progressive separation of the signals. This was done to make a qualitative analysis of operation.

Figures 20 through 22 shows the progressive delay of the $\underline{X}$ encoder as seen from the $\underline{X}^{-1}$ decoder during simultaneous operations. The output waveform is the summation of the auto-correlation and the cross-correlation. Figure 20 is the worst-case scenario where the signal peak is not added upon by the residual cross-correlation to increase the output magnitude. However, the main signal peak is still distinguishable from the residual voltage. The main peak is twice the amplitude of the next highest peak.

Figure 21 shows the $\underline{X}$ encoder input is delayed by eight time intervals. In this case, the main signal peak is 248 mV while the maximum residual voltage is 76 mV, thus maintaining a 4:1 ratio.

In Figure 22 the $\underline{X}$ encoder input is delayed enough so there is no overlapped information. This figure clearly shows the auto-correlation of the $\underline{X}$ sequence and the cross-correlation of the $\underline{X}$ and $\underline{Y}^{-1}$ sequences.

Figures 23 through 25 depict the progressive delay of the $\underline{X}$ encoder input as seen from the $\underline{Y}^{-1}$ decoder during simultaneous operations. At least a 2:1 ratio of signal to residual voltage is maintained.

In Figure 25 the $\underline{X}$ input is delayed to produce no overlap of information. It is easy to see the auto-correlation of the $\underline{Y}$ sequence and the cross-correlation of the $\underline{X}$ and $\underline{Y}^{-1}$ sequence.

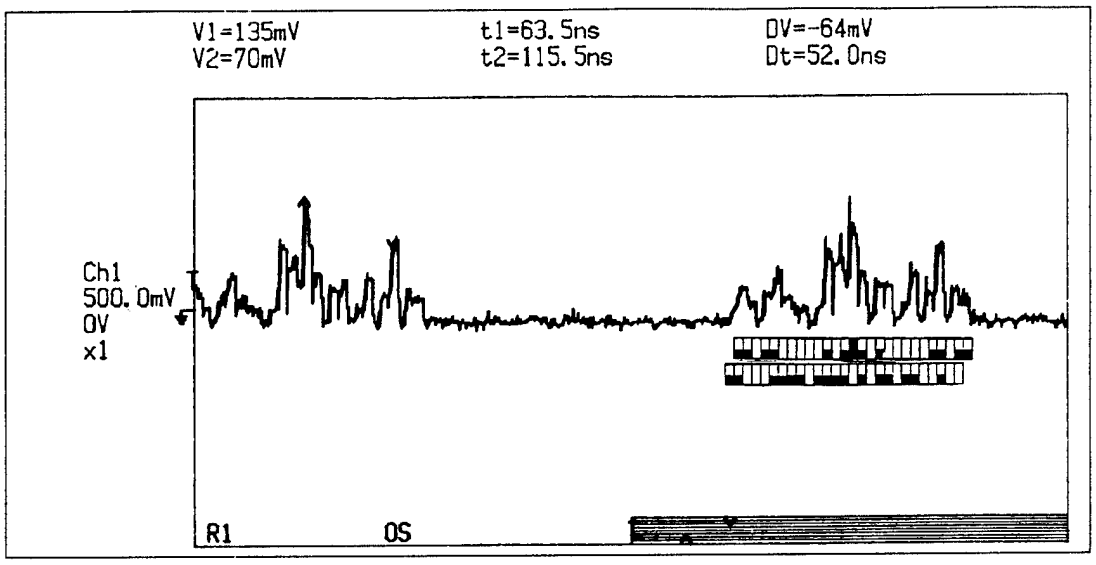

Figure 20 Simultaneous Operation from $\underline{X}^{-1}$ Decoder (5 ns Delay).

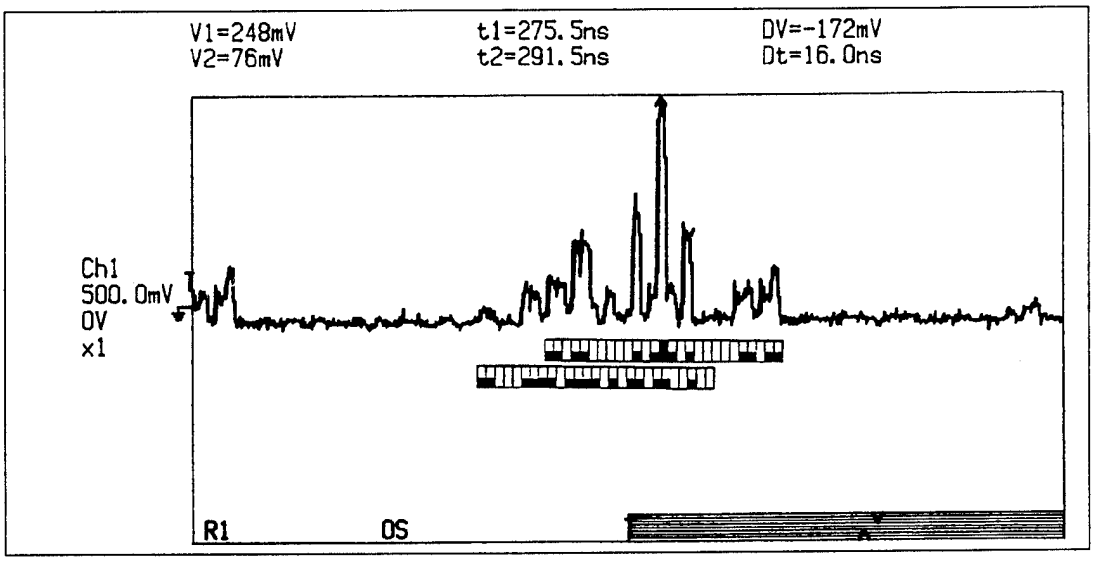

Figure 21. Simultaneous Operation from $\underline{X}^{-1}$ Decoder (40 ns Delay).

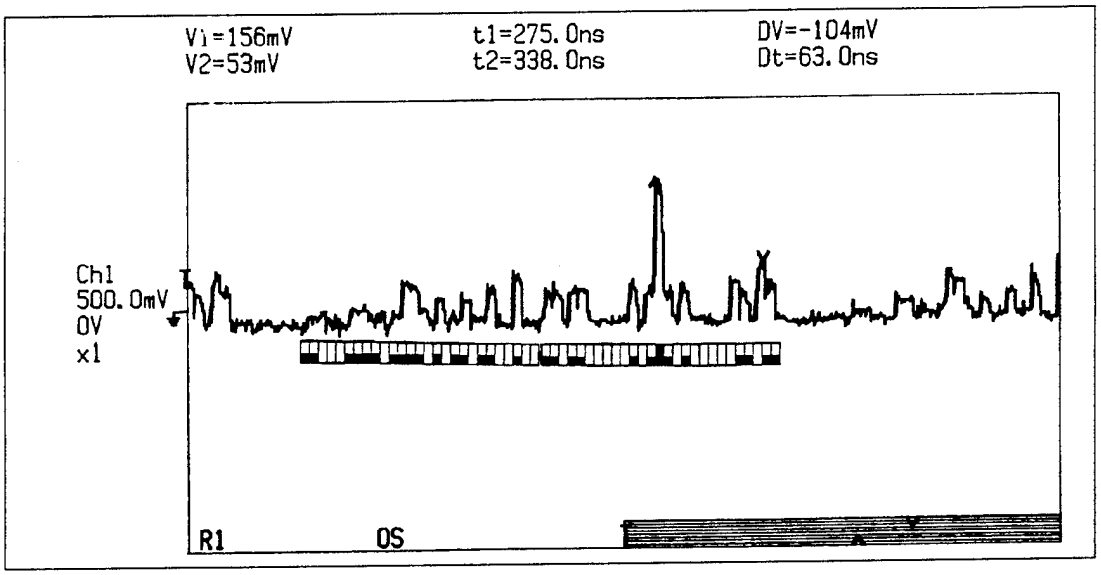

Figure 22. Simultaneous Operation from $\underline{X}^{-1}$ Decoder (90 ns Delay).

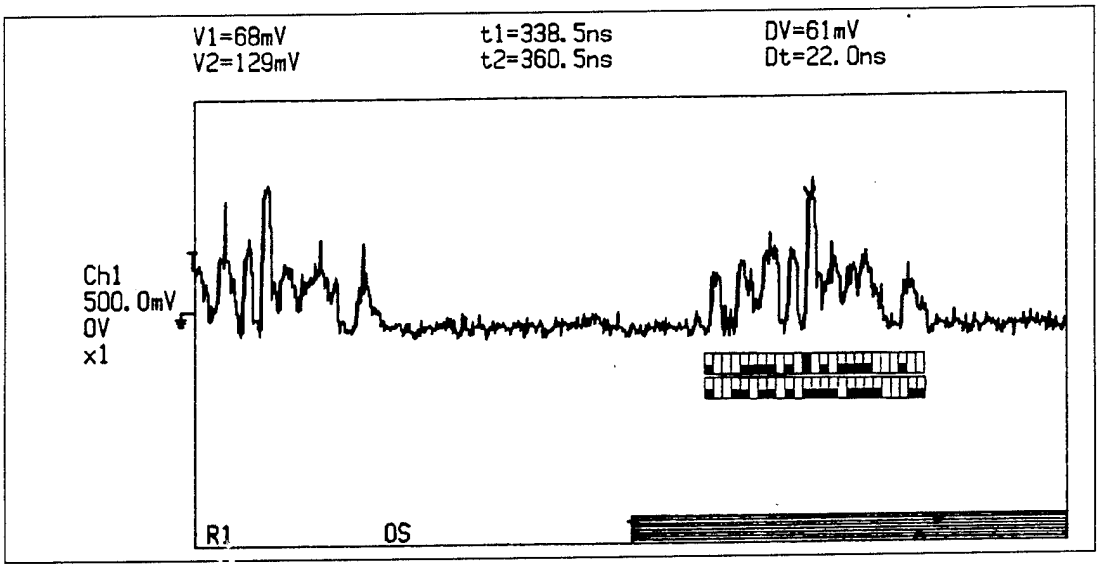

Figure 23. Simultaneous Operation from $\underline{Y}^{-1}$ Decoder (no Delay).

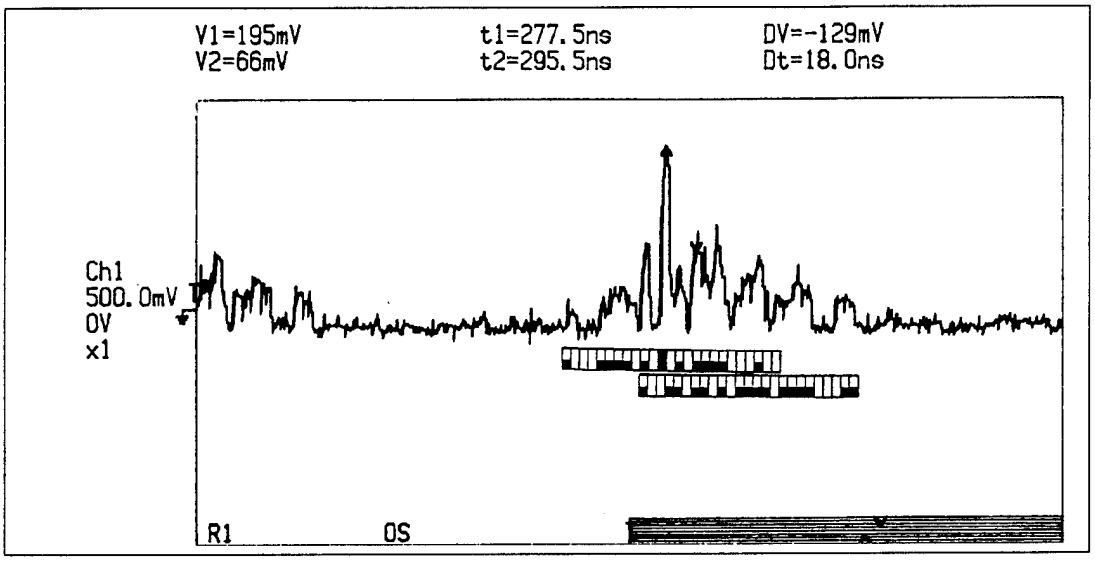

Figure 24. Simultaneous Operation from $\underline{Y}^{-1}$ Decoder (45 ns Delay).

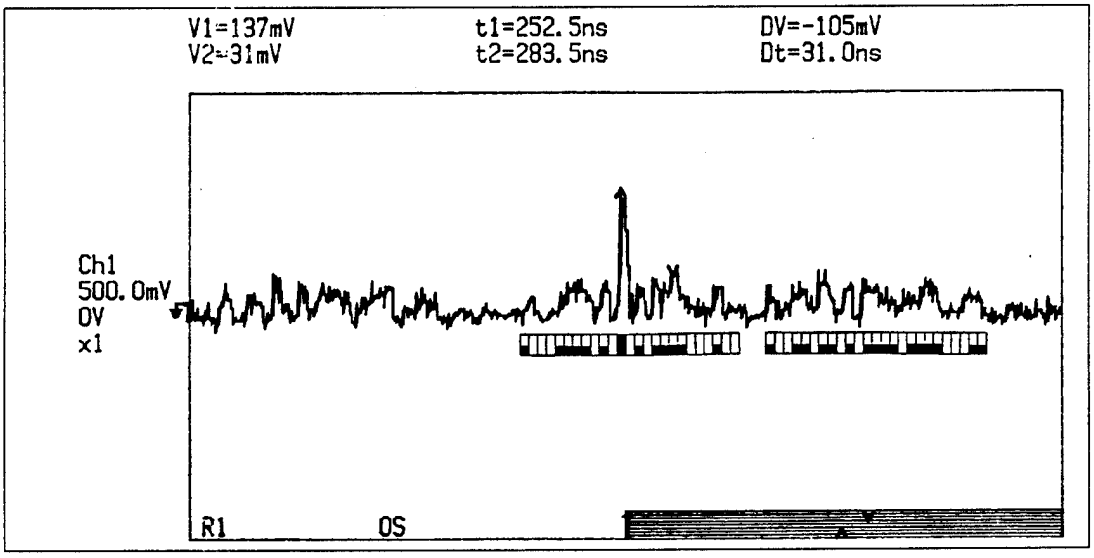

Figure 25. Simultaneous Operation from $\underline{Y}^{-1}$ Decoder (90 ns Delay).

Where the signal appears in Figure 22, the corresponding position in Figure 25 shows no information and vice versa. This shows the asynchronous access for each user during simultaneous operations. The analysis in this section demonstrates the encoders and decoders function properly during simultaneous operations.

D. THRESHOLD DETECTOR

Restating the objective, CDMA is to provide asynchronous access and, most importantly, reproduce the input signal at the receiver end. From Figures 22 and 25 it is clear to see that these waveforms do not look like the single input pulse with a width of 5 ns. By using a threshold detector, a threshold voltage level can be selected to pass only the main signal peak and reject the residuals.

Figure 26 is the schematic of the detector used. Because the pulse width of the signal is so narrow (5 ns), an ECL comparator was used. For high speed communication equipment ECL is used because of the 1 ns edge speeds and propagation delays along with

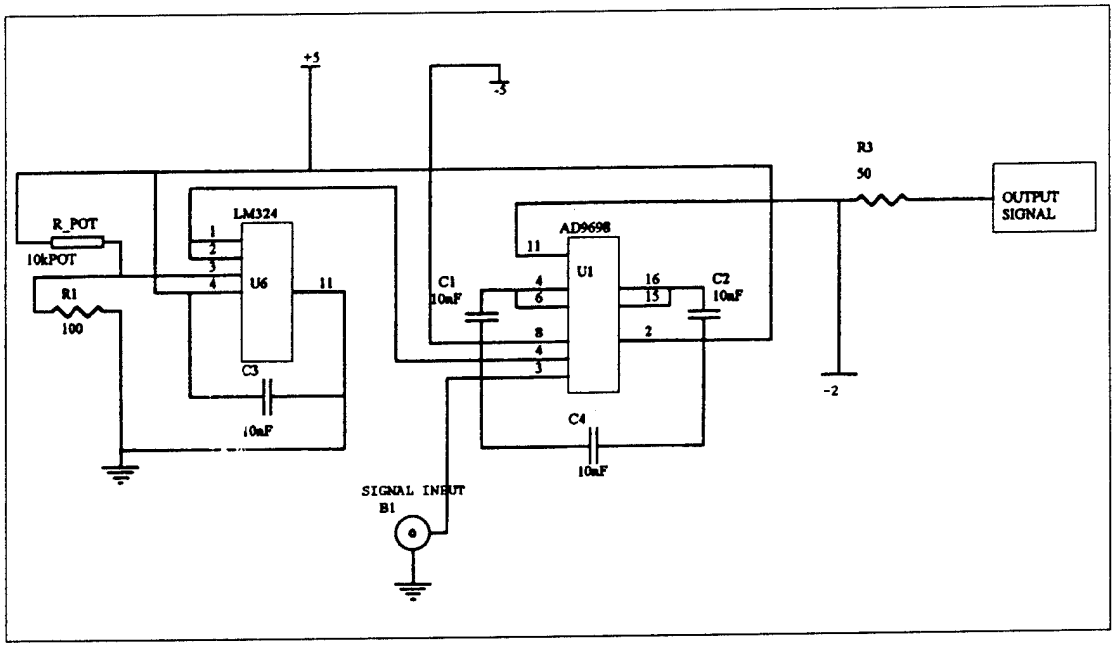

Figure 26. Schematic of Threshold Detector.

greater than 500 MHz flip-flop toggle rates. The output swing for a typical transfer curve varies from a low state of -1.75 V to a high state of -0.9 V with respect to ground. In this case the low state or "0" is -1.0 V, while the high state "1" is -0.9 V. A threshold voltage of 80 mV was selected due to the highest residual voltage being at 76 mV (Figure 21).

Figure 27 is the output of the threshold detector when the input is Figure 22. This looks very much like the input signal. The output is from the ECL family and, therefore, a bipolar output waveform with a negative DC bias is expected. The output has a pulsewidth of 5 ns. Figure 28 is the result of having the input of Figure 25. The signal was fed back into the bit error detector. When the input/output voltage threshold and the input delay were adjusted, the signal was reconstructed without any errors.

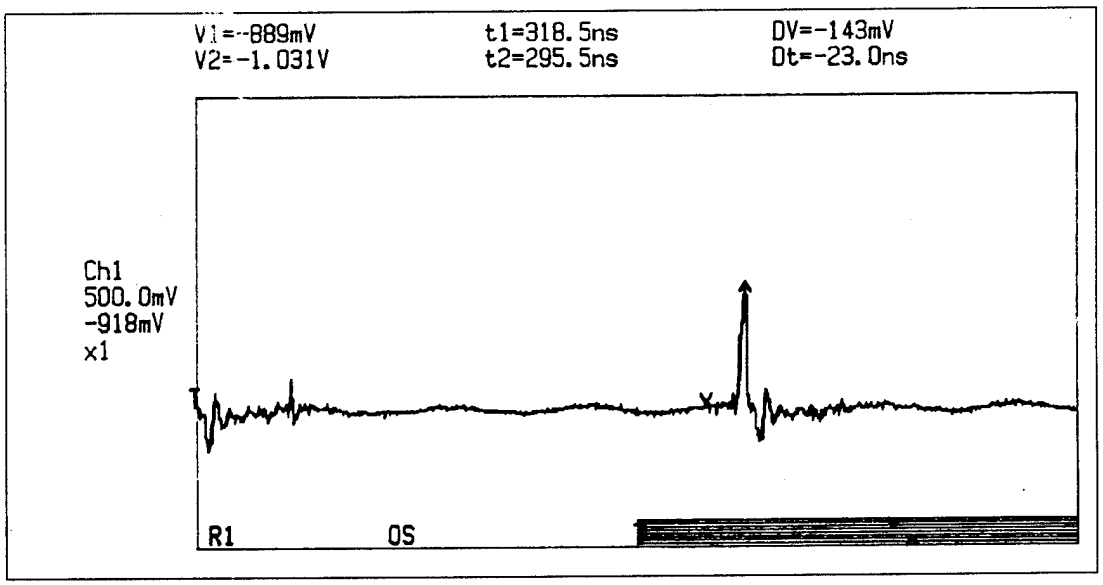

Figure 27. Output of Threshold Detector from Input of Figure 21.

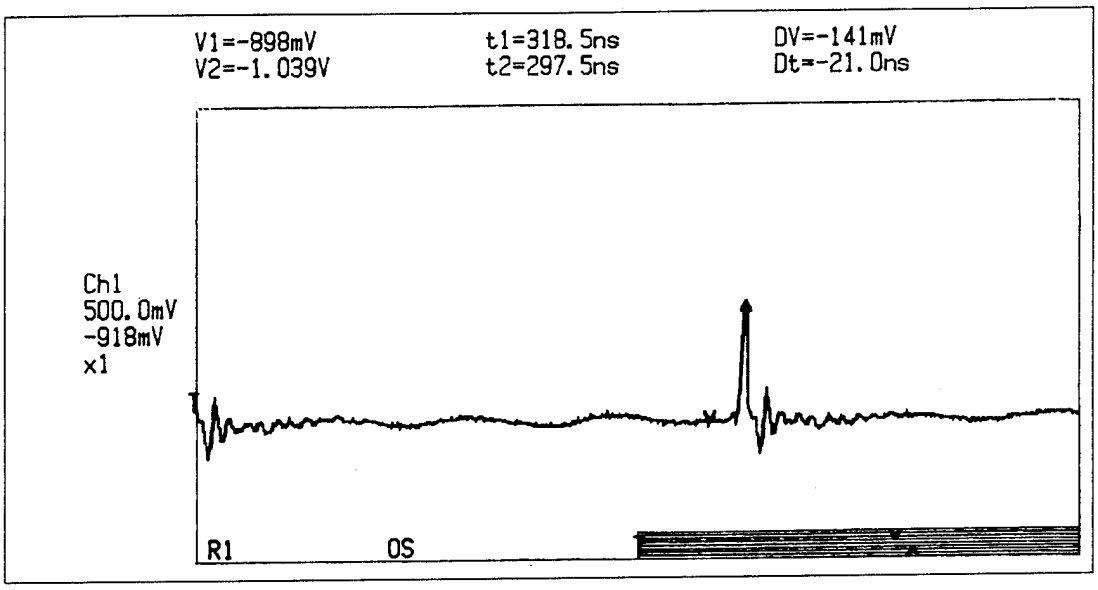

Figure 28. Output of Threshold Detector from Input of Figure 24.

Up until now, the input signal has been kept simple for easy analysis. Although the single input pulse works very well, it does not make a very interesting communication signal. This section will look at a more complicated input signal.

Figure 29 shows the output waveform from an input of six ones separated by three zeros (1000 1000 1000 1000 1000 1000). Figure 30 is the output of the threshold detector when in input is the waveform shown in Figure 29. From this figure it is easy to see the side lobing rejection and that the signal is cleaner. A band diagram was place beneath the waveform and it is clear that the pulses are aligned.

Figure 31 shows the theoretical output of the auto-correlation for the six pulse sequence. One important note to make is the triangular shape of the correlation function. Comparing the output from the threshold detector with the theoretical value, it is clear to see that these signals are the same input signal placed under the waveform. The triangular shape of the output is characteristic of the auto-correlation function. This data does confirm the encoders and decoders are still performing as expected with a more complicated signal.

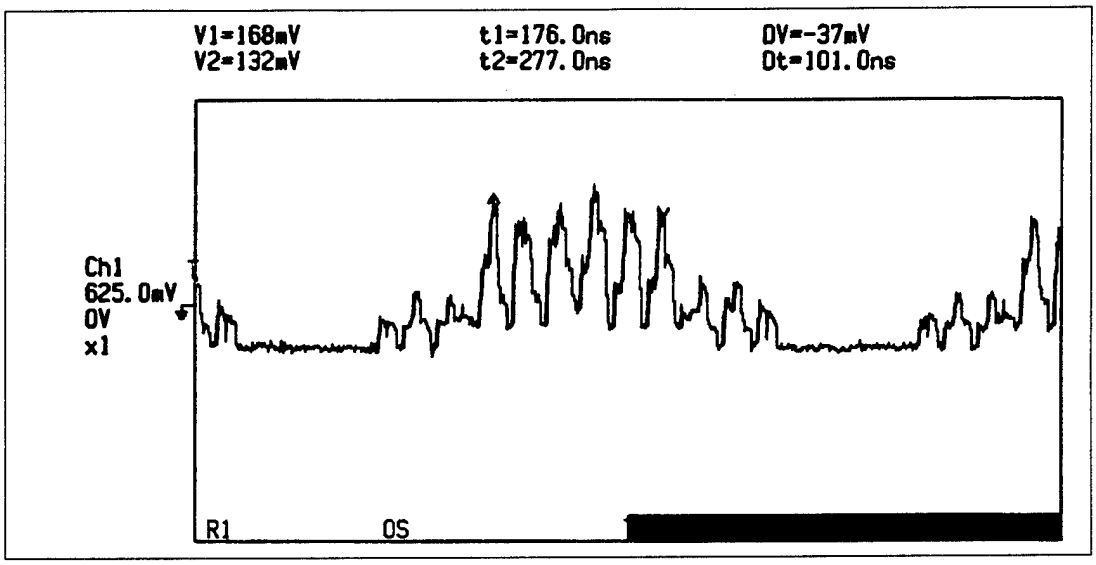

Figure 29. Auto-Correlation Output from Six Pulse Input.

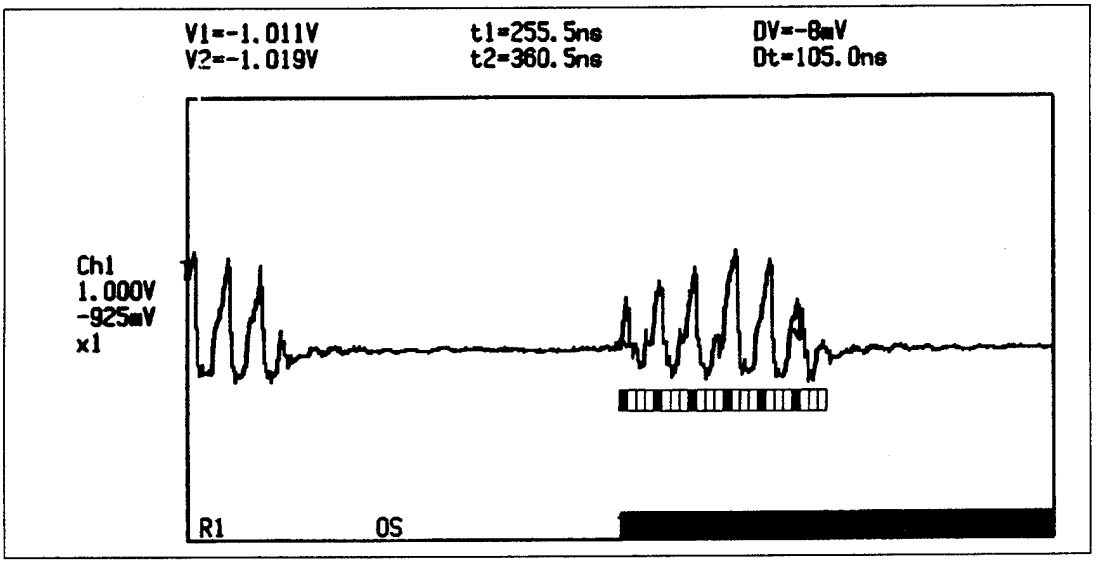

Figure 30. Output from Threshold Detector with Figure 29 as Input.

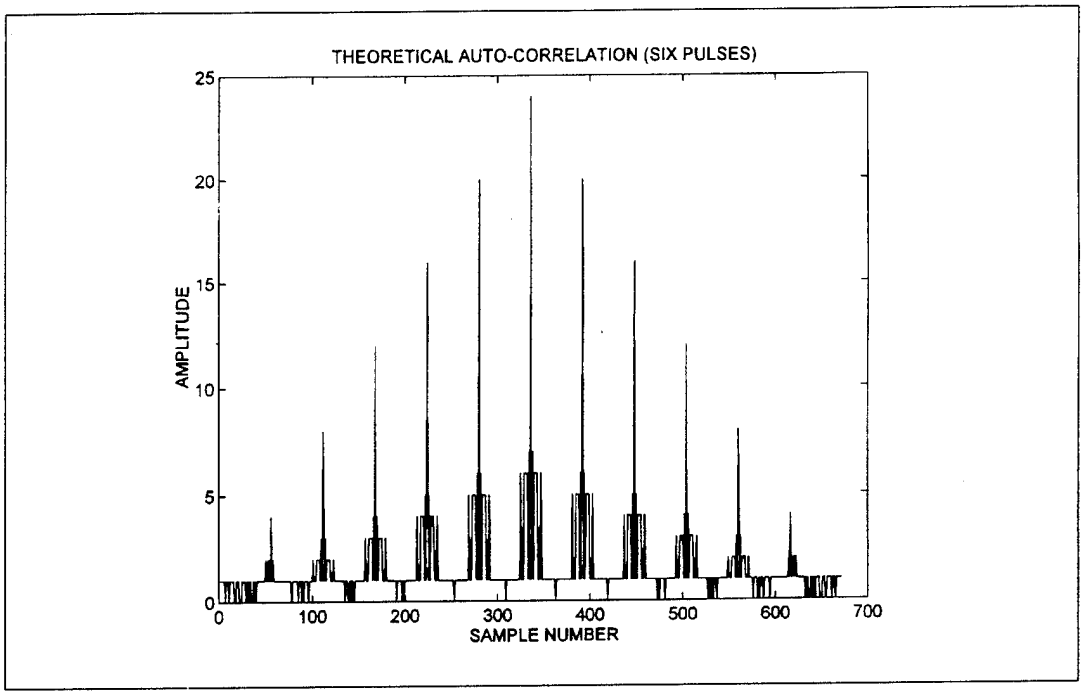

Figure 31. Auto-Correlation Output from Complicated Input.

The input signal is further complicated by a selecting an input signal of (1100 1010 0010 1001 0000 1000 0000 10000). Figure 32 is the auto-correlation of this complicated signal. Figure 33 is the output of the threshold detector. This particular sequence was chosen to show the effect of pulses occurring in numerous different position is a single word. The performance of this FO-CDMA system depends on the number of zeros between each one. Figure 33 shows the more zeros between the pulses, the more distinguishable the signal becomes.

The code "weight" used for this experiment was four, and therefore a four-to-one ratio was achieved for the signal-to-residual power (auto-correlation). This ratio should be improved by increasing the code "weight"; however, there is also an increase in the coincidence of pulses between the correlated waveforms. This effect increases the probability of error (Figure 33). It turns out that as long as the code "weight" of the sequence is less than the number of users, the probability for error is held to a minimum. For further discussions on the probability of error, see References [1], [2], [7] and [8].

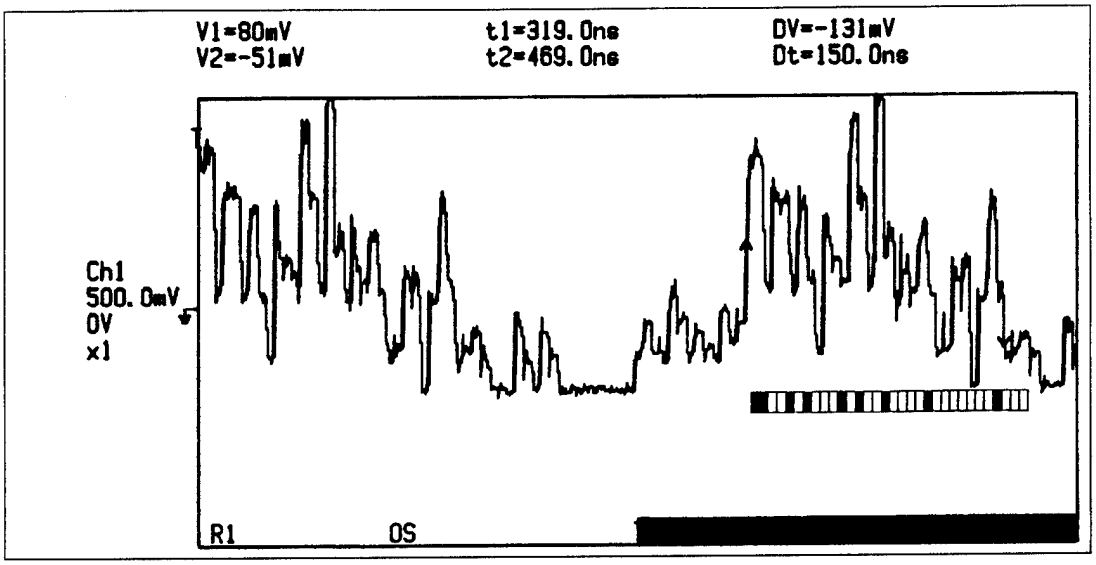

Figure 32. Auto-Correlation Output from Complicated Input.

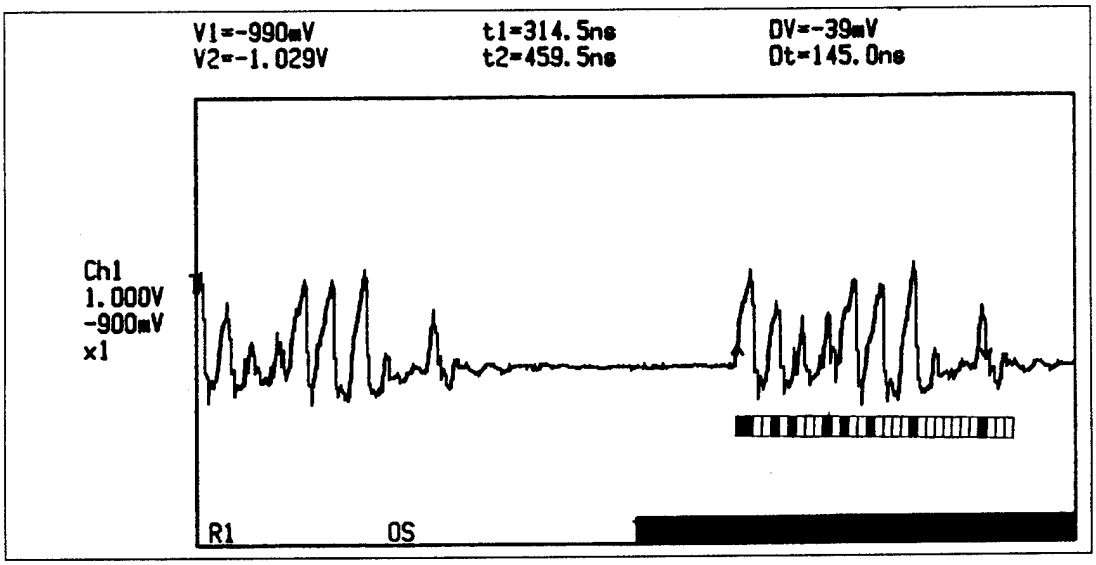

Figure 33. Output from Threshold Detector with Figure 31 as Input.

VII. SUMMARY

Optical-fiber transmission is rapidly replacing copper cable, due to its ability to handle large amounts of information at low cost. Although the available bandwidth to transport information is immense, the system's capacity is bottlenecked by electronic interfaces for the desired signal processing.

This thesis examines fiber-optic code division multiple access system in which low information data rates are mapped into high rate address codes (signature sequences), to achieve asynchronous communications free of network control among many users. The class of signature sequences used are called "optical orthogonal codes." The (0,1) sequence code sets were used in pulse code operation. The code sets have a minimal pair-wise cross-correlation and offset auto-correlation used with on-off pulse waveforms.

Once the optical orthogonal codes were established, the codes were implemented into the encoders and decoders. The optical delay lines were constructed for both encoders and decoders to provide the necessary pulse spacing in the output sequences. The implementation of these pure optical components perform all signaling processing functions optically. The electronic conversion is done sparingly, thereby exploiting the extremely large bandwidth of the optical fiber.

In this experiment the auto-correlation and cross-correlation properties of the optical orthogonal codes were demonstrated with good results. The construction of this system was relatively easy with only one problem to note. The components used in the construction of the system do not posses uniform losses and, therefore, the power loss management became a major concern. The components had to be connected in a particular combination such that amplitudes of the delay output were nearly uniform. The solution to this dilemma was to utilize a MATLAB program written by J.W. Andre [6] to optimize the selection of each combination.

The major system losses involve the number of users and the code "weight." These losses are strictly due to the implementation of the encoders and decoders and the network

fabric. As seen from the output of the threshold detector (Figure 33), discrimination of a complicated signal becomes increasingly difficult. This is a result of nearing the performance envelope of the ECL comparators in the detector. These comparators have a rise/fall time of approximately 2.6 ns. If the signaling pulsewidth is less than 5 ns, the comparators are unable to discriminate the signal from the noise. Most of the signal pulses are not rectangular in shape but rather triangular. Therefore, the pulsewidth depends upon the voltage threshold of the detector.

The advantages of fiber optic delay lines are not limited to their use in the kinds of structures that are encountered in a more traditional electronic technologies. Fiber optic lines offer precision timing capabilities and enormous transmission bandwidth. Rapid progress in the fields of fiber communication should ensure the further development of components that can exploit excellent properties of the optical fibers.

APPENDIX A. E/O CONVERSION CHART

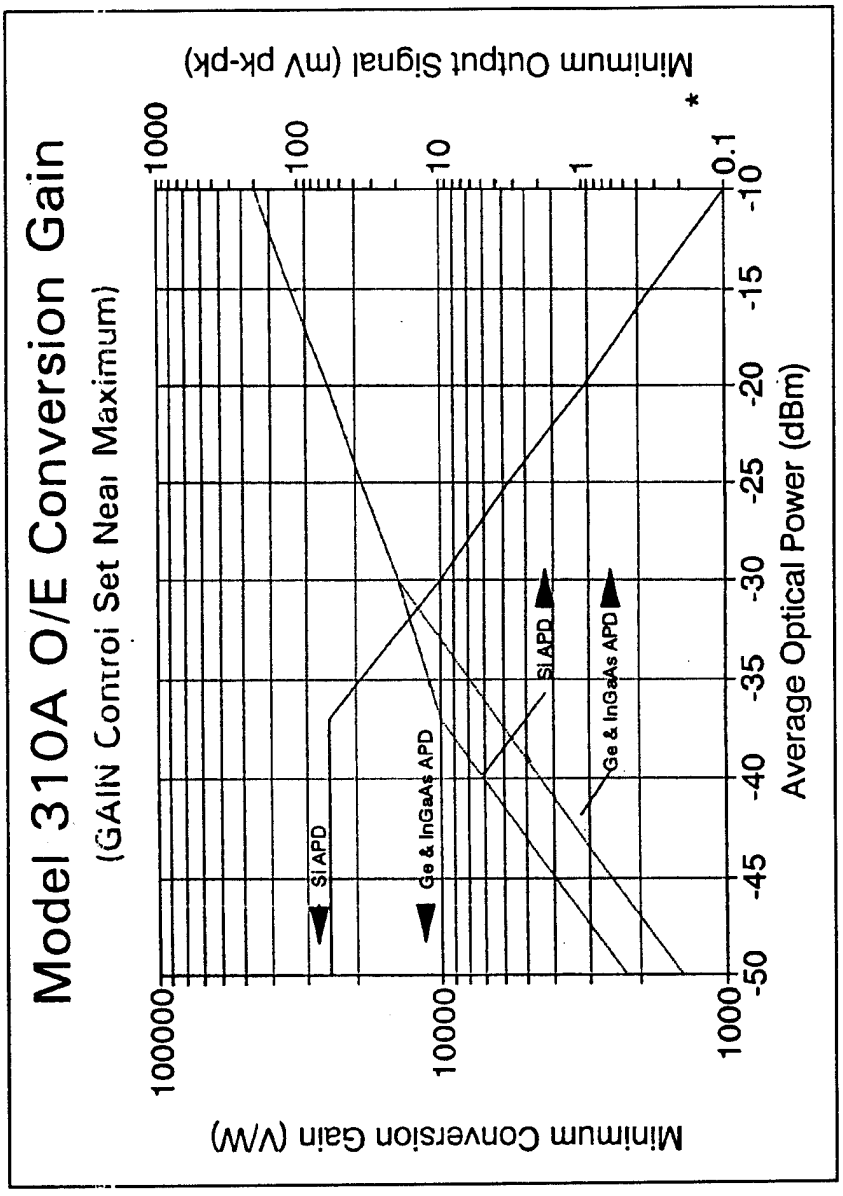

Figure 34. Electrical to Optical Conversion. [From Ref. 12: p. 8]

APPENDIX B. MEASURED SPLITTING LOSSES

The following is a summary of measured losses from the 1 x 4 and 4 x1 splitters used in this thesis.

MATRIX A (1x4 SPLITTER)

Measured losses (-dB)				
Device ID number	Input lead #1	Input lead #2	Input lead #3	Input lead #4
580	-8.2	-8.7	-8.2	-7.8
581	-8.5	-6.9	-8.4	-8.6
583	-7.3	-8.6	-7.3	-9.3
584	-8.6	-9.1	-8.2	-9.1
585	-8.5	-7.2	-7.7	-9.1
586	-7.2	-6.7	-8.1	-7.6
587	-8.2	-8.2	-8.9	-8.7
614	-10.1	-10.1	-8.7	-9.1

MATRIX B (4x1 SPLITTER)

Measured losses (-dB)				
Device ID number	Output lead #1	Output lead #2	Output lead #3	Output lead #4
580	-7.7	-7.9	-7.1	-7.2
581	-8.2	-7.1	-7.5	-8.4
583	-7.1	-8.2	-7.3	-9.2
584	-7.6	-8.2	-7.5	-8.1
585	-9.3	-6.9	-7.4	-9.4
586	-7.9	-7.4	-7.2	-8.2
587	-8.4	-8.3	-8.8	-9.3
614	-10.1	-10.1	-8.5	-9.8

APPENDIX C. MATLAB SOURCE CODE

Source code and data file for MATLAB sorting code. This program was written by Andre [6].

Splitt.dat - data file containing measured splitting losses.

```
**********************************************************************
7.7  7.9 7.1  7.2
8.2  7.1 7.5  8.4
7.1  8.2 7.3  9.2
7.6  8.2 7.5  8.1
9.3  6.9 7.4  9.4
7.9  7.4 7.2  8.2
8.4  8.3 8.8  9.3
10.1 10.1 8.5 9.8
8.2  8.7 8.2  7.8
8.5  6.9 8.4  8.6
7.3  8.6 7.3  9.3
8.6  9.1 8.2  9.1
8.5  7.2 7.7  9.1
7.2  6.7 8.1  7.6
8.2  8.2 8.9  8.7
10.1 10.1 8.7 9.1
```

RR.m - MATLAB function used to rotate right a row vector.

```
**********************************************************************
  function [x]=rr(y);
  l=length(y);
  z=zeros(size(l+1));
  x=zeros(size(l));
  z(2:l+1)=y;
  x(1)=z(l+1);
  x(2:l)=z(2:l);
```

Splitt.m - MATLAB source code used to find optimum component combination.

```
**********************************************************************
clear
load splitt4.dat;    % Load data file%
a=splitt4;           % Assign data to matrix variable "a"%
```

```
clear splitt4;          % Clear old variable%
b=[0 .4 .5 .7];         % Assign delay line losses to vector variable "b"%
S=2;                    % Assign an initial standard deviation to variable S%

for l=1:2               % Begin first loop through matrix%
  r1=a(l,:);            % Assign l row of matrix to variable "r1"%

for m = 1:2             % Begin second loop through matrix%
 r2=a(m,:);             % Assign m row of matrix to variable "r2"%

if l~=m                 % check for the same rows, bypass if equal%

  for i =1:4            % Begin first loop through row vector r1%
   r1=rr(r1);           % Rotate right r1 %
    s=r1+r2+b;          % Sum up vectors %
    x=std(s);           % Take standard deviation of vector %
    if x<S              % Test for lower value %
      S=x;              % Make assignments if true %
    ra1=r1;
    ra2=r2;
    ba=b;
  end

   for j = 1:4          % Begin second loop through row vector r2%
    r2=rr(r2);          % Rotate right r2%
    s=r1+r2+b;          % Sum up vectors%
    x=std(s);           % Take standard deviation of vector%
    if x < S            % Test for lower value %
      S=x;              % Make assignments if true%
      ra1=r1;
      ra2=r2;
      ba=b;
     end

   for k = 1:4          % Begin third loop through row vector b%
    b=rr(b);            % Rotate right r2%
    s=r1+r2+b;          % Sum up vectors%
    x=std(s);           % Take standard deviation of vector%
     if x<S             % Test for lower value%
      S=x;              % Make assignments if true%
      ra1=r1;
      ra2=r2;
      ba=b;
```

```
    end
   end
  end
 end
end
end

S              % Display results%
ra1
ra2
ba
```

LIST OF REFERENCES

1. Scholtz, R. M., "The Origins of Spread-Spectrum Communications," IEEE *Trans. Comm.*, vol. COM-30, no. 5, pp. 822-854, 1982.
2. Couch II, L. W., *Digital and Analog Communication Systems*, 4th ed., Macmillan Publishing Company, New York, 1993.
3. Schilling, D., Milstein, L., Pickholtz, R., Kullback, M., and Miller, F., "Spread Spectrum for Commercial Communications," *IEEE Comm. Mag.*, pp. 66-78, 1991.
4. Forschini, G. and Vannucci, G., "Using Spread-Spectrum in a High-Capacity Fiber-Optic Local Network," *IEEE Journal of Lightwave Tech.*, vol. 6, no. 3, pp. 370-379, 1988.
5. Mollenaur, L., "Solitons: the Future of Fibre Communications," *Physics World*, pp. 29-32, 1989.
6. Andre, John W., LT., United States Navy, "Feasibility Study of Implementing a Code Division Multiple Access Data Link Utilizing Fiber Optic Delay Lines," Naval Postgraduate School, Monterey, California, Master's Thesis, September, 1992.
7. Pruncal, M. R., Santoro, M. A., and Fan, T. R., "Spread Spectrum Fiber-Optic Local Area Network Using Optical Processing," *IEEE Journal of Lightwave Tech.*, vol. LT-4, no. 5, pp. 547-554, 1986.
8. Tamura, S., Nakano, S., and Akazaki, K., "Optical Code-Multiplex Transmission by Gold Sequences," *J. Lightwave Technol.*, vol. 3, no. 2, pp. 121-127, 1985.
9. Khansefid, Fahad, Gagliardi, Robert, and Taylor, Herbert, "Design of (0,1) Sequences for Pulsed Coded Systems," Prepublication manuscript submitted May 7, 1990 to IEEE *Trans. Comm.*
10. Textronix, *RTD 720A Transient Digitizer*, User Manual, Textronix Inc., 1992.
11. Hewlett Packard, *71600 B Pattern Generator/Error Detector*, User Manual, Hewlett Packard, 1992.
12. Broadband Communications Products, *310A High Gain, Wideband O/E Converter*, User Manual, Broadband Communication Products Inc., 1993.

INITIAL DISTRIBUTION LIST

		No. Copies
1.	Defense Technical Information Center Cameron Station Alexandria, Virginia 22304-6145	2
2.	Dudley Knox Library, Code 52 Naval Postgraduate School Monterey, California 93943-5101	2
3.	Chairman, Code EC Department of Electrical and Computer Engineering Naval Postgraduate School Monterey, California 93943-5121	1
4.	Professor John P. Powers, Code EC/Po Department of Electrical and Computer Engineering Naval Postgraduate School Monterey, California 93943-5121	2
5.	Professor Ronald Pieper, Code EC/Pr Department of Electrical and Computer Engineering Naval Postgraduate School Monterey, California 93943-5121	1
6.	Naval Command, Control and Ocean Surveillance Center RDT&E Division Attn: M. Brininstool, Code 946 San Diego, California, 92151-5000	1
7.	Lieutenant Kenneth J. McKown 1532 Coronado Avenue San Diego, California 92154	1